TU Clausthal

Materialwissenschaft und
Werkstofftechnik

Band 3/02

Mikhail Popov

Enhancement of mechanical properties of different magnesium alloys due to grain refinement by severe plastic deformation processing

Professor Dr. rer. nat. habil. Yuri Estrin

Institut für Werkstoffkunde
und Werkstofftechnik

Enhancement of mechanical properties of different
magnesium alloys due to grain refinement
by severe plastic deformation processing

Dissertation

ZUR ERLANGUNG DES GRADES EINES

DOKTOR-INGENIEURS

VORGELEGT VON

Dipl.-Ing. Mikhail Popov

AUS TYNDA

GENEHMIGT VON DER

FAKULTÄT FÜR NATUR- UND MATERIALWISSENSCHAFTEN

DER TECHNISCHEN UNIVERSITÄT CLAUSTHAL

TAG DER MÜNDLICHEN PRÜFUNG:

31.10.2007

Die Arbeit wurde am Institut für
Werkstoffkunde und Werkstofftechnik
der Technischen Universität Clausthal angefertigt

Vorsitzender der Promotionskommission:	Prof. Dr. A. Wolter
Hauptberichterstatter:	Prof. Dr. Y. Estrin
Berichterstatter:	Prof. S.V. Dobatkin
	Prof. H. Palkowski

Hiermit versichere ich, dass ich diese Arbeit selbständig angefertigt habe und keine weiteren außer den angegebenen Hilfsmitteln verwendet habe.

Mikhail V. Popov

I. Literature review

I.1. Severe Plastic Deformation

Severe Plastic Deformation (SPD) is the advanced method using different non-conventional techniques to obtain ultrafine-grained (UFG) materials.

To have a better and explicit understanding the definition of UFG materials and SPD processing will be given here according to a key article composed by the leading experts in this field from all over the world past year 2006 [I.1]. The first publications about the production of bulk UFG materials by SPD processing have appeared in the literature in the early 1990s and many papers followed avalanchelike so that there was some necessity to formally define the widely used terms within the field.

Firstly the UFG materials will be considered. Any material is pretending to use this indication in case it conforms to the following requirements:

- it is a polycrystal having very small grains with an average grain sizes less than ~1 μm

- microstructure should be fairly homogeneous and reasonably equiaxed with a majority of the grain boundaries having high-angles of misorientation

So, the grain sizes of UFG materials lie within the submicrometer – 100-1000 nm and nanometer – less than 100 nm, ranges. The small grain size together with the homology of the microstructure defined by the second criterion allows to achieve advanced and unique properties typical for the UFG materials [I.2].

The SPD processing characterizes various experimental procedures of metal forming that may be used to inflict very high strains on materials leading to exceptional grain refinement. Following features refer to SPD:

- high strain is imposed without any significant change in the overall dimensions of the workpiece

- deformation is carried out under considerable hydrostatic pressure

Since some scientists have found the roots of the SPD already in ancient China [I.3] the most important early contribution for the

modern world of SPD is the work of Segal and co-workers in Minsk [I.4] where the technique of equal-channel angular pressing (ECAP) was first introduced in the form now used everywhere.

From that time SPD processing was becoming an important research area having a significant potential for use in a wide range of industrial applications. Thus numerous SPD processing techniques were devised and several of them became major, so the short overview of the most auspicious and interesting ones among them will be listed here.

Equal-Channel Angular Pressing

ECAP is the most advanced SPD technique at a present. It was developed by Segal and co-workers at 1972 in Minsk (Belarus) [I.4 and 5]. In Fig. I.1 the process is shown schematically. The main idea is to press a metal workpiece through a channel which is bent at an abrupt angle. The deformation itself occurs in the intersection plane of the two parts of the channel, so called entry channel and exit channel. Since the cross-sectional dimensions of the workpiece remain unchanged, the pressings can be and usually are repeated to accumulate exceptionally high strains in the material. The equivalent strain, ε, introduced in ECAP is determined by a relationship between the angle between the two parts of the channel, Φ, and the angle representing the outer arc of curvature where the two parts of the channel intersect, Ψ.

$$\varepsilon = \frac{1}{\sqrt{3}}\left(2\cdot\cot\left(\frac{\Phi}{2}+\frac{\Psi}{2}\right)+\Psi\cdot\alpha\right), \alpha = \csc\left(\frac{\Phi}{2}+\frac{\Psi}{2}\right) \quad (I.1)$$

Here N is the number of passes through the die. This formula is given in [I.6] and in the literature the simpler form can be found, where $\alpha = 1$ [I.7].

Usually the value of the angle Φ lies in the range 90° – 140°. The angle Ψ is smaller and as a rule lies between 0° and 30° [I.8 and 9]. In majority of the cases the dies have Φ and Ψ equal to 90° and 0° respectively, so that the equivalent strain achieves 1.15 per one ECAP pass.
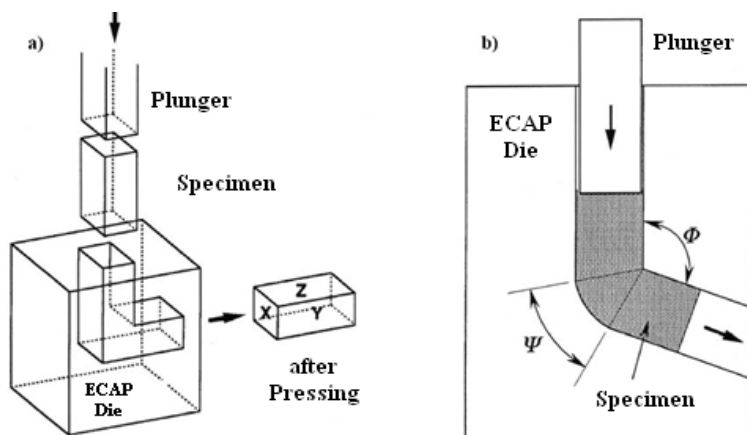
Fig. I.1 ECAP die schematically

Another remarkable feature of the ECAP processing is the possibility of rotating the billet about its longitudinal axis between each pass, Fig. I.2. This leads to four basic processing routes [I.10]:

- Route A with no rotation

- Route B_A or B_C – the rotations are 90° in alternate or same direction, respectively

- Route C with 180° rotation [I.11]
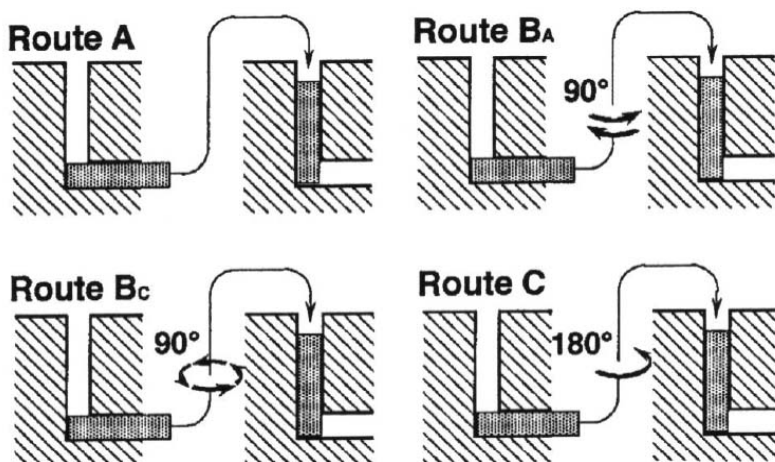
Fig. I.2 ECAP routes [I.12]

Using these routes different slip systems can be activated which leads to the diverse resulting textures. And they are responsible for the various mechanical properties of the same material though pressed under equal parameters but using a different route. In Fig. I.3 the principles of the shearing evolution during ECAP processing are shown.

If we imagine that the workpiece is an elementary cell and it stretches itself each time after one ECAP pass in the direction of the shearing then during route B_C it is returning into its original shape, thus introducing the most homogeneous deformation into the material. And, for example during the Route A the elementary cell i.e. microstructure are becoming more and more stretched along the shearing direction. So, generally the Route B_C is used to achieve the microstructure consisting of homogeneous and equiaxed grains with grain boundaries having high angles of misorientation.
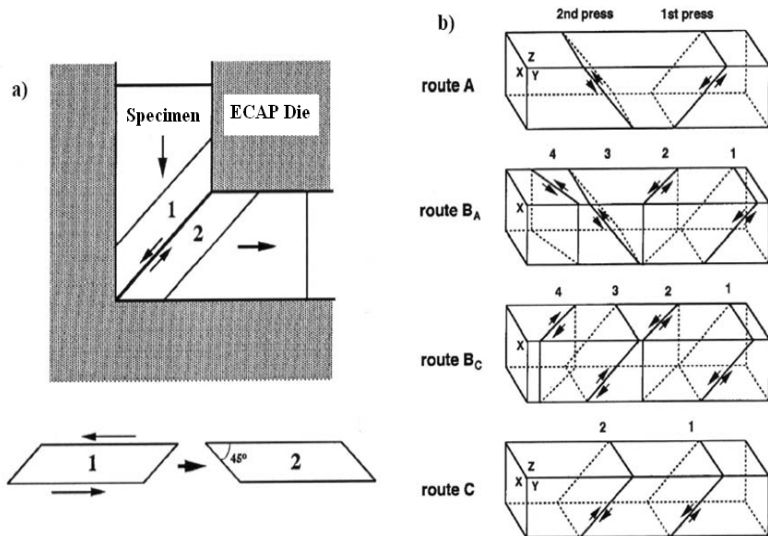
Fig. I.3 Shearing during ECAP [I.7 and 12]

The very important things that make ECAP to a real ECAP and not to a complicated bending are the friction conditions in the channel and the presence of the high hydrostatic pressure which is provided through a back pressure [I.13]. Since the whole deformation occurs in the shearing plane it is very important to have a plane and not a spread deformation zone, Fig. I.4.
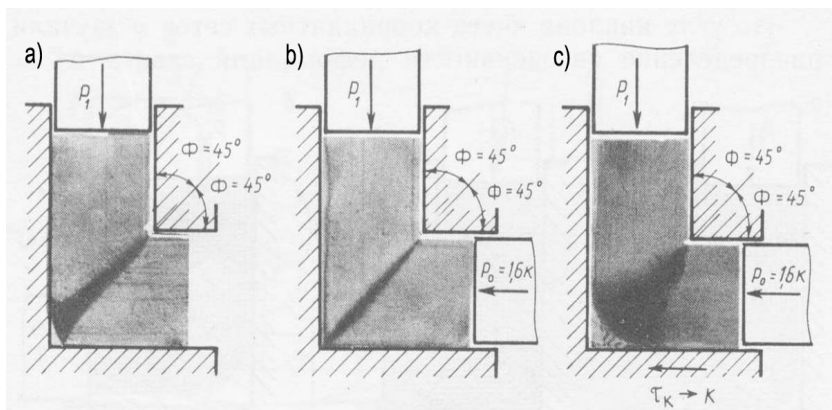
Fig. I.4 Deformation zone at different ECAP parameters [I.13]

The usual situation during ECAP without providing any back pressure can be observed in Fig. I.4.a), where the deformation zone looks like a half-fan. It should be considered that even if the grease is added in the entry channel the friction still is not completely removed and the deformation zone may spread to a fan-like form, as shown in c). This, a), kind of processing takes place if the billet can be extracted from the die after each pass, for example when the die consists of two halves and can be opened or the billet can be pushed out of the die by the extra plunger, for instance. Anyway it is very complex and time-consuming, though there are some advantages as it will be shown later (see also Ch. II). The variant c) itself with the slight back pressure and high friction is typical if the specimens are pressed one after each other. During such a "conventional" ECAP pressing the die is not supposed to be opened after each pass and the next billet just presses out the previous one which plays the role of a back pressure in the exit channel. But such a back pressure is discontinuous, not strong enough and uncontrollable. It is discontinuous, because the back pressure force is based on the friction that the already pressed billet performs in the exit channel hindering the next billet to come through. And this friction is getting lower as the pressed billet comes out of the exit channel.

In both cases there is a possibility of formation of so-called "dead zone" when the material does not go through the inside corner, but shapes a rounding which also disturbs the proper plane geometry of the deformation zone. It occurs during ECAP processing without back pressure if the material does not fill the corner a) or in case with back pressure if the material fills the corner but it breaks off and stays there c).

Anyway the transformation of the shearing plane into any other geometry leads to the inhomogeneous strain and as a consequence to the "low quality" microstructure. The latter may be still refined but the mechanical properties will be much lower. One of the examples is shown in this work behalf the superplastic properties of AZ31 (see Ch. IV).

The back pressure also gives a possibility to reduce the processing temperature without cracking or destroying the material, thus suppressing the possible grain growth or any recrystallization and recovery processes and keeping microstructure very fine. It is highly important for the materials needed to be pressed at higher temperatures, which are brittle at room temperature due to the lack of slip systems – Mg, for example or the ones, that are simply too hard to press – Ti, steel.

So it is very important to have a proper die design and adequate pressing parameters, sometimes they may even differ from one material to another. Since it is more specifically it will be discussed in the Chapter II, where the ECAP rigs and pressing parameters are described.

High-Pressure Torsion

The sample during High-Pressure Torsion (HPT) usually has a form of a thin disk and is subjected to torsional straining under pressure, Fig. I.5 [I.14]. An ingot is held between anvils and strained under the applied pressure, P of several GPa, Fig. I.5 a). A lower holder with the specimen located within a cavity rotates and the surface friction forces deform the sample by strain. In spite of large strain values the deformed sample is not destroyed due to the high hydrostatic pressure [I.8]. In order to achieve pressures higher than 2 GPa a modified geometry with cavities in each anvil is generally used, Fig. I.5 b) [I.15].

If there is no outward flow of material, the disk thickness remains constant and the true torsional strain, γ, is given by

$$\gamma = \left(\frac{r}{h}\right) \cdot \varphi$$
,

where r is the distance from the center of the disk, φ is the torsional angle in radians, and h is the sample thickness. In case there is some outward flow of material between the two anvils and a corresponding reduction in the value of h an alternative relationship has been developed [I.14].
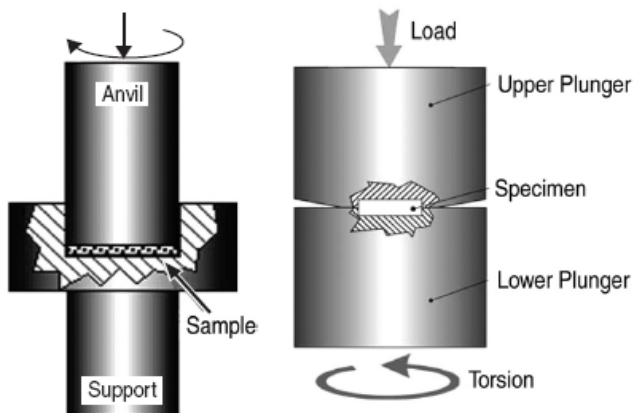
Fig. I.5 The principle of HPT, a) – tool with the sample located within a cavity in the support anvil and b) – tool with cavities in both anvils [I.1]

To compare the shear strain value during torsion with a strain during deformation by other schemes the former value is usually converted into so-called equivalent strain, ε, which can be calculated using the following relation:

$$\varepsilon = \left(\frac{1}{a}\right) \cdot \gamma$$

where a takes either the values from a plastic flow criterion equal to 2 for Tresca and to $\sqrt{3}$ for von Mises or from the Taylor theory for polycrystals, whereas a = 1.65 for texture-free face-centered cubic (fcc) metals and decreases slightly to lower values during continued deformation [I.1].

The grain refinement and microstructure changes happen in the first line away from the center of the disk. But after several rotations the deformation by the given mode often results in the similar refinement of the microstructure in the center of samples. The microhardness measured across the whole diameter of the sample exhibits usually uniform values after several rotations as well [I.8].

The possible problems for the SPD via HPT may emerge during processing of hard-to-deform or brittle materials, where sliding between an anvil and a sample or cracking of the latter is possible. Generally, the imposed pressure should be increased to remove these drawbacks. However, such a solution leads to additional technological

difficulties. Therefore it is necessarily to use more strong material for anvils and optimize a die set design.

<u>Other SPD techniques</u>

Numerous techniques for SPD processing are available and their number increases rapidly with the time. Many of them have proven their capability for the fabrication of UFG materials. Among them are ECAP, HPT, ARB, MDF, TE, CEC and RCS [I.1]. ECAP and HPT were already mentioned above. ARB, accumulative roll-bonding, as well as RCS, repetitive corrugation and straightening make use of conventional rolling facilities, thus showing the potential of producing nanostructured materials in a continuous and economical way. The process of multi-directional forging (MDF) assumes multiple repeats of free-forging operations including setting and pulling with changes of the axes of the applied load. Both twist extrusion (TE) and cyclic extrusion and compression (CEC) use a straight die, which form changes differently with its longitudinal direction. Another interesting method named STSP, severe torsion straining process, was recently developed and represents a continuous process for grain refinement without requirement of any die [I.16].

Another family of SPD methods arises from ECAP by scaling it up using multipass [I.17] or rotary die [I.18 and 19] or a side-extrusion facility [I.17]. The principles of ECAP processing may be incorporated into conventional rolling using the conshearing [I.17], continuous confined strip-shearing (C2S2) [I.17] or equal channel angular rolling (ECAR) [I.20].

In the following section the results about SPD via ECAP and HPT on magnesium alloys will be considered and the microstructure and mechanical properties evolution will be discussed.

I.2.   Overview of mechanical properties and microstructure of Mg alloys processed
via HPT and ECAP

<u>Mg-RE</u>

ECAP was performed on the magnesium alloy ZW1101 containing about 1wt% of Y: Mg-11wt%Zn-0.9wt%Y, by Zheng et al. [I.21-23]. The Mg-Zn-Y alloys are strengthened by a quasicrystalline icosahedral phase – I-phase. It has a chemical composition of Mg_3YZn_6 and is formed as a second phase in the α-Mg matrix during

conventional solidification. Quasicrystals are isotropic and possess quasiperiodic lattice structure. Since the dislocations can not move easily in quasicrystals they are hard and strong, so can be used as reinforcement in the metallic alloys. However, the icosahedral phase in Mg-Zn-Y system is formed as a coarse eutectic structure on solidification. To use the I-phase as a strengthening phase, it must be distributed finely in the alloy. To separate and disperse the I-phase and to reduce the grain size in the α-Mg matrix the conventional extrusion and SPD through ECAP were used.

The microstructure and mechanical properties of this material were investigated on as-cast and after different thermomechanical treatments: as-cast + ECAP [I.21 and 22], as-cast + extrusion and as-cast + extrusion + ECAP [I.23].

The ECAP of as-cast ZW1101 alloy has significantly refined the grain size of α-Mg, broken and dispersed the I-phase. The grain size was reduced from 150-250 µm down to 4-8 µm after 4 passes [I.21] and from 60-100 µm down to 3-4 µm after 8 passes [I.22]. The eutectic I-phase was broken into fine particles with size of 0.5-1 µm in both cases. The microstructure after 8 passes exhibited more homogenous grains than after 4 passes. After extrusion the grain size of the alloy was already 12 µm but it was further refined by ECAP down to 0.5 µm after 8 passes [I.23].

The ECAP was very effective in the improvement of tensile properties of the ZW1101 alloy but they were inferior to those obtained by conventional straight extrusion [I.23], in spite of the finer matrix grain size after ECAP. After 8 ECAP passes the as-cast material had a yield stress of 160 MPa, ultimate stress of 287 MPa and the elongation of 26%, while the extruded cast material obtained 273 MPa, 376 MPa and 19% respectively [I.22]. Microhardness of the extruded alloy followed by ECAP was increased from 82 up to 88 Hv already after 2 passes and did not change significantly through the last 6 passes [I.23].

The same situation with tensile properties was observed in a similar alloy with a lower Zn content: Mg-5wt%Zn-0.9wt%Y-0.2wt%Zr [I.24]. The ECAP was performed on as-cast and on as-extruded state. The ultimate stress of the ZWK510 alloy after extrusion was about 360 MPa with 12% elongation and in as-cast state after 8 ECAP passes the alloy exhibited only 300 MPa and 15% respectively. After the texture analysis it was observed, that the as-extruded material has a fiber texture and the texture of ECAPed material consists of high intensity basal planes inclined about 45° to the extrusion direction.

Hence the higher elongation and lower yield strength and ultimate strength obtained by specimens after ECAP.

The mechanical properties of the alloy WZ73 (Mg-6.8wt%Y-2.5wt%Zn) followed by ECAP were studied in [I.25-27]. Yield strength of 293 MPa, tensile strength of 350 MPa and elongation of 18% were achieved at an initial strain rate of 1×10^{-2} s^{-1} at room temperature. The grain size after ECAP was 1.6 µm. The yield strength was almost unchanged up to 200 °C and at 300 °C the superplastic elongation of over 300% was observed [I.26]. It was suggested, that the second phase formed in the α-Mg matrix of the WZ73 alloy strongly depends on the cooling rate during solidification but apart from its composition it serves to pin the grain boundaries, thus the enhanced thermal stability [I.27].

In [I.28-32] the magnesium alloy containing 10wt%Gd was investigated after SPD through HPT. After the processing the samples obtained a homogeneous UFG structure with an average grain size less than 100 nm. It was found that the grain size remains virtually unchanged up to 265 °C. The microhardness value of the Mg-10wt%Gd was increased from 715 MPa in coarse-grained state up to 1050 MPa after HPT and further enhance up to approximately 1300 MPa was observed after annealing at 250 °C possibly due to the start of precipitation of fine particles. The UFG samples of the alloy have demonstrated superplasticity with an elongation to fracture equal to 580% at 400 °C and deformation rate of 10^{-3} s^{-1} [I.32].

The properties of MA8 alloy with composition Mg-1.5wt%Mn-0.3wt%Ce were investigated after ECAP [I.33]. The mean grain size was 0.3 µm in two different states, with equilibrium and non-equilibrium grain boundaries. The yield stress, ultimate stress and elongation to failure were 210 MPa, 250 MPa and 11% for the former state and 225 MPa, 260 MPa and 2% for the latter state, respectively. So, the non-equilibrium condition of grain boundaries lowers the ductility but enhances the strength properties. At 127 °C yield stress decreases to the value of 70 MPa and further reduce is observed. Elongation to failure of >150% was achieved at 180 °C and 5×10^{-4} s^{-1}.

It is apparent, that the magnesium alloys with rare earth elements and the impact of SPD on them have been barely studied. Moreover the magnesium alloys only diluted by RE elements were processed exceptionally by HPT and not by ECAP. Mechanical properties were not investigated at higher temperatures and the precipitation processes and their influence on the strength of the alloy were not reported.

Mg-Li

Alloying magnesium with lithium of extremely low density, 0.534 g/cm3 allows further weight reduce and helps to overcome such a problem as poor formability and raises strength. A basic parameter – specific elastic modulus E/ρ – is one of the important factors considered in designing light vehicles. Comparison of this parameter for Fe, Ti or Al with the one for Mg alloys specifically Mg-Li alloys shows nearly 20% of advantage for the latter [I.34]. According to the Mg-Li phase diagram with Li content between 5 and 11 wt.%, bcc structured β phase of Li solid solution will co-exist with the hcp α phase of Mg solid solution, what seems to be very favorable for the superplasticity.

The texture of the Mg-3.3wt%Li alloy after two different ECAP routes A and B_C was investigated in [I.35 and 36]. The strong sheet and shear textures were observed after route A and B_C respectively. The texture modification during ECAP was responsible for the lower yield stress and higher ductility after route B_C. The yield stress of the material processed via route B_C was 95 MPa versus 115 MPa via route A. The ductility was vastly improved and reached 35% after route B_C. The other remarkable feature was the different extents of recrystallization for different pressing routes, namely the partially recrystallized structure resulted in the mean grain size of 2.6 μm after route A and fully recrystallized structure with homogenous and equiaxial grains of 3.4 μm after route B_C.

The superplastic behavior after ECAP was studied on the Mg-8wt%Li [I.37 and 118] and Mg-8.5wt%Li [I.18] alloys deformed through ECAP. The former alloy was EX-ECAPed in [I.118] through a die with Φ = 110° at relatively low temperature of 200 °C for two passes after extrusion and already exhibited ~970% at 200 °C. The authors followed the tendency and augmented the die angle Φ up to 135° with Ψ equal to 20° thus getting the alloy easily pressed up to 10 passes at room temperature without any surface cracking, which seems to be the first publication for a magnesium alloy ever processed successfully by ECAP at ambient temperature [I.37]. The highest elongation to failure of ~1780% at the testing temperature of 200 °C using an initial strain rate of 1.5×10^{-4} s^{-1} was achieved in this investigation after EX-ECAP and is the record one for the group of Mg-Li alloys. Such a high ductility is ascribed to the restricted grain growth during the pressing due to the processing by ECAP at room temperature, which resulted in grain size measured to be about 1-3 μm.

Three types of alloys were used in [I.38] study: $\alpha+\beta$ dual phase Mg-8wt%Li-1wt%Zn – LZ81 and Mg-10wt%Li-1wt%Zn – LZ101 alloys and

β single phase Mg-12wt%Li-1wt%Zn-1wt%Ca – LZC1211 alloy, to which Ca was added to prevent coarsening of recrystallized grains during ECAP and heat treatment. The best tensile strengths were observed at room temperature by LZ81 after ECAP, namely yield stress of 195 MPa, tensile strength of 225 MPa and large elongation of 45%. Whereas alloy LZ101 exhibited even larger elongation to failure, which was equal to 90% at room temperature. Comparable tensile properties but with lower ductility were achieved for Mg-8wt%Li-1wt%Al – LA81 after ECAP at 130 °C [I.39]. The reported grain size in LA81 for α phase is ~500 nm and even ~200 nm for the β phase.

In the other work [I.40] the superplastic behavior of LZ101 at low temperatures was investigated by Yoshida et al. The ECAPed material was tested at the temperature of 100 °C using the strain rate of 3×10^{-5} s^{-1} and a worthy elongation to fracture of 421% was obtained. Using the results of this work as a goal a group of scientists performed a comprehensive study of five alloys finding out the mechanical properties at room and elevated temperatures after ECAP [I.34 and 41]. These alloys were Mg-11wt%Li-1wt%Zn – LZ111, Mg-9wt%Li-1wt%Zn – LZ91, Mg-9wt%Li-1wt%Zn-0.2wt%Mn – LZM910, Mg-9wt%Li-1wt%Zn-1wt%Al-0.2wt%Mn – LZAM9110 and Mg-9wt%Li-3wt%Al-1wt%Zn-0.2wt%Mn – LAZM9310. However all the results were inferior in comparison to the mechanical properties observed at room temperature in [I.38] and to the superplasticity from [I.40].

It was shown that for the whole bunch of alloys processed in [I.34, 38-41] the ECAP process can only refine grains of each phase, but can not change the dispersion of the phases significantly. The β phase can be refined faster than the α phase and has a lower grain size. The α phase was usually refined to ~0.5 μm. The β phase due to its bcc morphology has more independent slip systems and can accommodate the most deformation. Compared to the β phase in α+β phase titanium alloys the former contributes to superplastic deformation in Mg-Li alloys [I.40].

Mg-Zr

The addition of zirconium into pure magnesium enriches the latter with fine particles and this may serve to retain an ultrafine grain size at the elevated temperatures required for superplastic flow. And truly, most of work on the magnesium alloys containing Zr was oriented to find the proper processing routes in order to achieve superplasticity.

The elongation to failure of about 420% at an initial strain rate of 3.3×10^{-4} s^{-1} at the testing temperature of 300 °C was obtained in Mg-0.6wt%Zr after extrusion and only one pass of ECAP at the same 300 °C [I.42]. The presence of the particles is effective in keeping a grain size of ~70 µm in the cast condition and the grain size was further reduced to ~11 µm after extrusion. The following ECAP processing helped to reduce the grain size down to ~1 µm and it stayed reasonably stable up to 300 °C [I.17]. Another alloy of a very close composition Mg-0.55wt%Zr in as-extruded condition was undergone an ECAP pressing at 240 °C but the grain size was reduced only to 8.6 µm [I.43]. The superplastic properties were much lower as in [I.17 and 42] which is considered with the coarser microstructure obtained after SPD in [I.43].

The alloy with following composition Mg-7.5wt%Al-0.2wt%Zr was processed due to EX-ECAP for 2 passes at 200 °C with the resulting grain size of ~0.8 µm [I.44 and 45]. Superplastic elongations of 750±30% were attained in the range of temperatures from 175 to 225 °C using an initial strain rate of 3.3×10^{-4} s^{-1}. In order to increase the elongation to failure at higher strain rates, additional ECAP processing was conducted at 250 °C for 2 passes prior to ECAP at 200 °C for 2 passes. These two additional passes led to the augmentation of high-angle boundaries from ~65% to ~90% and the consequence was the overall increase of ductility in the high strain rates range of 10^{-1}-10^{-2} s^{-1}. For example elongation to fracture was enhanced from ~240% to ~340% at a strain rate 1×10^{-2} s^{-1} at the temperature of 225 °C after the additional processing.

Mechanical properties at room temperature of the Mg-3wt%Zn-0.5wt%Zr – ZK31 alloy were investigated after ECAP and subsequent annealing at different temperatures [I.46], different ECAP conditions [I.47] and after ECAP and subsequent rolling [I.48]. The best combination of properties was achieved for ECAPed material after 4 passes with subsequent annealing with tensile strength of 310 MPa, yield strength of 265 MPa and elongation to failure equal to 18% [I.46]. The grain size was measured to be approximately 1 µm. Slightly lower tensile and yield strengths were observed for the materials in cast + rolled and ECAP + rolled conditions, however with significantly lower ductility [I.48]. The texture measurements were performed in [I.47 and 48] after ECAP. For route B_C and for the route using following rotations 180° and 90° after each extrusion was found that the high density basal planes are parallel to the extrusion direction which makes the basal slip difficult to occur. As a result the highest tensile and yield strengths but poor ductility are obtained after ECAP in [I.46]: 340 MPa, 310 MPa and 6%, respectively.

ZK40 – Mg-3.7wt%Zn-0.6wt%Zr was investigated for superplastic behavior at low temperatures [I.49-52]. The elongation to failure of the alloy processed by ECAP for 4 passes tested at 250 °C and strain rate $1x10^{-4}$ s^{-1} was 660% [I.50]. The mean grain size was measured to be 0.8 μm.

Exceptionally high tensile ductility of commercial magnesium alloy ZK60 – Mg-5.8wt%Zn-0.6wt%Zr is reported in [I.53 and 54]. It was achieved by ECAP without any extra processing steps. The tensile ductility at 220 °C was 2040% and 1400% for the strain rates of $3x10^{-4}$ s^{-1} and $3x10^{-3}$ s^{-1}, respectively. It is the highest elongations found not only for Mg-Zr alloys but among the Mg alloys generally. Microstructural observations revealed bi-modality, which may be responsible for the superplastic behavior observed. The large grains as fragmentations of large initial grains by twins were in the size about 12.5 μm and small recrystallized grains were about 1.8 μm. But the small grain population itself may be considered to be a mixture of two fractions: relatively large grain, ~4 μm, and very small ones, ~0.4 μm. So the grain structure after the ECAP processing became effectively tri-modal. Twinning in the first passes of ECAP was considered to be a crucial factor in triggering dynamic recrystallization in the following passes and obtaining a fine grain size in the small grain population. Numerous studies confirm the great potential for superplastic behavior of this alloy processed by ECAP, though with different results: >250% [I.55 and 56], >550% [I.57], >800% [I.58 and 59], >1000% [I.60 and 61], >1300% [I.62].

The effect of ECAP on the hydrogen absorption/desorption properties of ZK60 was studied in [I.63]. It was shown, that ECAP represents a promising processing technique for developing new hydrogen storage materials with enhanced hydrogen desorption kinetics.

A ZK60 alloy was subjected to SPD also by HPT at ambient temperature [I.64]. Microhardness was as high as 1700 MPa and the microstructure resulted in nanometerscale grains.

Mg-Al-Mn

Properties of AM60, Mg-6wt%Al-0.2wt%Mn processed by ECAP were studied in [I.65 and 66]. In the die with the Φ angle equal to 120° it was possible to press the material up to 10 passes by 150 °C. Grain size was successfully reduced down to 1 μm and following properties were attained, yield stress 230 MPa, ultimate tensile stress 310 MPa and elongation to failure 15%. The precipitates of $Mg_{17}Al_{12}$ phase were observed in the alloy. According to the Mg-Al phase diagram they are supposed to be stable up to 462 °C [I.66]. But after differential

scanning calorimetry (DSC) measurements the temperature associated with dissolution of $Mg_{17}Al_{12}$ particles was defined to be 390 °C for as-cast material [I.65]. For the material after ECAP the peak related with dissolution of $Mg_{17}Al_{12}$ particles was even lower than in as-cast condition, 360 °C. It was considered, that the microstructure was distorted during ECAP, so that the dissociation of particles at lower temperature was possible.

Mg-Al

Only two articles are describing magnesium alloys after SPD diluted simply by aluminum. In [I.67] the grain size of the Mg-0.9wt%Al processed by ECAP was reduced down to 17 μm. Both yield strength and elongation to fracture were increased up to 140 MPa and 15%, respectively, at an initial strain rate of $3.3x10^{-4}$ s^{-1}.

The higher Al content in the alloy Mg-9wt%Al led to the smaller grain size after EX-ECAP, namely 0.7 μm [I.68]. The EX-ECAP is a processing route when the ECAP is carried out on the preliminary extruded material, which resulted in exceptionally high tensile ductility in the Mg-9wt% Al alloy with elongations to failure up to 840% even at testing temperature as low as 200 °C (~0.55 Tm) at an initial strain rate of $3.3x10^{-4}$ s^{-1}.

The addition of Zn into this system leads to the biggest family of alloys processed by ECAP or other SPD methods.

Mg-Al-Zn

The composition of the alloy AZ61 is Mg-6wt%Al-1wt%Zn. The alloy processed by EX-ECAP exhibited exceptional superplastic properties including a maximum elongation of 1320% after pressing through four passes when testing at 200 °C with an initial strain rate of $3.3x10^{-4}$ s^{-1} [I.44 and 69]. A lower elongation of 1190% was observed in [I.70].

Mechanical properties were reported in [I.71-76]. High properties were obtained in [I.71 and 72] with the tensile strength equal to 400 MPa, yield strength equal to 220 MPa and elongation of 15%. Maybe the stress-strain curves were made in true coordinates, so the high ultimate tensile strength. Generally, excellent ductility at room temperature can be attained through ECAP for this alloy: 55% [I.74-76] and 33% at initial strain rate of $1x10^{-3}$ s^{-1}, 67% at a lower strain rate of $1x10^{-5}$ s^{-1} and still 14% at high strain rate of $1x10^{-1}$ s^{-1} [I.73]. The measured grain size after ECAP was usually less than one micrometer, approximately 0.5 μm but in [I.74-76] it was reduced only

to 8.4 µm, which can be ascribed to the pressing conditions and high ECAP temperature of 275 °C.

Microstructure [I.77-79], damping values [I.80 and 81], mechanical and superplastic behavior [I.18-19, 58-59, 81-88] after SPD through ECAP of AZ91 – Mg-9wt%Al-1wt%Zn sometimes with addition of 0.2wt%Mn were studied. Different ductility with elongations to failure over 300% [I.18-19, 85-86] and over 500% [I.58-59 and 87] were reported. However elongations to failure more than 900% were achieved only in [I.84] and [I.88] at 200 and 250 °C, respectively, using initial strain rate of $7x10^{-5}$ s^{-1} in both cases. In [I.84] the ECAPed material and the same one but with subsequent annealing were tested for low temperature superplasticity. The grain size directly after ECAP at 175 °C was about 0.7 µm and grain boundaries were in a non-equilibrium state. After annealing at 225 °C for 12 hours the grain size was increased up to 3.1 µm and non-equilibrium grain boundaries were changed to equilibrium grain boundaries. The elongations were 661% [I.82-84] and 956% [I.84] of the ECAPed and annealed material, respectively. The lower superplastic elongation for the as-ECAPed material probably arises because dislocation movement is hampered by the long-range stresses associated with the non-equilibrium grain boundaries and grain boundary sliding, which is crucial for superplasticity. Grain boundary sliding is less accommodated for the as-ECAPed material, compared to the annealed one. Another point of view concerning the state of the grain boundaries and their influence on the superplasticity is given in [I.58 and 59], where the elongation to failure of 570% was attained at 300 °C and using a relatively high strain rate $3x10^{-3}$ s^{-1}. The grain size was reduced as well to 0.8 µm. Here grain boundary diffusion was enhanced due to the presence of non-equilibrium grain boundaries and this grain boundary diffusion enhancement greatly assisted strain accommodation at grain triple junctions during superplastic deformation thus promoting superplasticity.

Properties of the AZ91 were investigated at room temperature in [I.81, 85, 86 and 88]. A very high tensile strength of 420 MPa and yield strength of 400 MPa were obtained after ECAP with decreasing temperature, i.e. the first pass made at 265 °C and the last one, the eighth made at 150 °C [I.88]. The grain size was 0.5 µm. However, the ductility of this sample was very poor – only 2%.

The majority of the articles written about SPD of magnesium alloys studying the effect of ECAP on microstructure and mechanical properties is about AZ31 alloy with 3wt% of Al and 1wt% of Zn. Beside usual mechanical properties such characteristics as superplasticity,

that will be discussed more thoroughly in Chapter III, fracture toughness and fatigue properties were investigated.

The value of plain-strain fracture toughness, K_{IC} was found to be larger after ECAP with grain size of 5 μm, than of the extruded material or material after ECAP with following annealing. This was ascribed to the finer grain size due to ECAP [I.89 and 90]. In [I.91 and 92] the ECAPed sample exhibited a lower crack growth rate but also a lower fatigue limit compared to the unECAPed sample due to the finer grains and lower yield strength, respectively.

Mechanical properties were investigated widely and by many work groups. The optimal thermomechanical processing for enhancing of the mechanical behavior is still not found and geometry of the ECAP tool and ECAP parameters themselves differ from one research to another. Thus it is difficult to define which material benefited for 100% from ECAP, so the papers with the highest achieved tensile strength, yield strength and elongation to fracture will be listed separately.

The ultimate tensile strength of approximately 300 MPa is a very high value attained after ECAP at moderate temperatures, where all the passes or the last one were made at 180-220 °C [I.91-95]. The grain size is usually reduced down to 2-3 μm. Such a high value of tensile strength is usually equal or superior to the one of the as-extruded material, with the average grain size of 20-30 μm. The tensile strength of 360 MPa was obtained in [I.71 and 72] with yield stress of 200 MPa and 18% of elongation. The grain structure was found to be bi-modal with a half of the grains smaller than 5 μm and the other half lying in the range of 5-10 μm. However, the look and developing of the curves is akin to the typical true stress-strain curves, which may be the reason of the outstanding result in strength.

The yield strength after ECAP was often measured to be much lower than 200 MPa. In [I.96], [I.97] and [I.46, 98-101] though, the yield strength of ≥200 MPa was reported by poor – <10%, moderate – ~15% and high – ~30% ductility, respectively. Values of tensile strength, yield strength and elongation to failure obtained in [I.98 and 99] were measured at a strain rate of 5×10^{-4} s^{-1} and are 300 MPa, 280 MPa and 28%, respectively. These values may be considered as the best simultaneous enhancement of strength and ductility for AZ31 alloy due to grain refinement via ECAP processing. The ultra-fine grain size of 0.5 μm has been produced utilizing a two-step ECAP: the first 4 passes at 225 °C and the fifth at 180 °C.

Very high elongations to failure at room temperature with more than 45% were reported in numerous works [I.102-112], thus suggesting

the advantage of ECAP processing regarding the naturally poor ductility of magnesium alloys. As a rule, the high ductility is accompanied by a very low yield stresses in the range of 100-140 MPa which were usually twice or even threefold [I.106 and 107] lower than the related ultimate tensile stresses. The record elongation to failure of 80% at room temperature was achieved by annealing at 300 °C for 80 min of the ECAPed specimen pressed at 250 °C for 6 passes [I.110]. Initial strain rate for this tensile test was set as $5x10^{-4}$ s^{-1}. The yield stress of this fine-grained material was only 90 MPa and after a large work-hardening the tensile strength reached 220 MPa.

To understand such contradictory results it is necessary to take a look into the microstructure and texture development during SPD via ECAP processing. According to [I.113] during the first ECAP pass dislocations are arranged into dislocations boundaries and sub-grain boundaries, corresponding to the low energy dislocation's, LED, theory. Then, these sub-boundaries evolve to low angle grain boundaries, LAGBs and high angle grain boundaries, HAGBs, which is a kind of continuous dynamic recovery and recrystallization (CDRR). The KiKuChi-line examination shows that the misorientation frequency below 5° decreases and the misorientation frequency higher than 15° increases for number of passes from one to eight. Whereas the grain refinement occurs effectively up to 4 passes and afterwards only the increase of HAGBs fraction takes place. No new recrystallization nucleuses surrounded with HAGBs were observed by TEM. But in [I.114 and 115] after shear bands and dislocation pile-ups were formed within grains a continuous recovery arises due to heating, leading to rearrangement of dislocations and formation of sub-grain structures as well as nucleation of new strain free grains within shear bands.

So the grain refinement mechanism for magnesium alloys during ECAP is defined by a combination of mechanical shearing, subsequent continuous recovery, recrystallization and grain and sub-grain cells growth [I.114]. The temperature plays a key role in texture evolution and effectiveness in the grain refinement of Mg by ECAP in addition to the processing route and amount of induced strain [I.114].

The process of plastic deformation itself in Mg and Mg alloys is highly anisotropic, since magnesium has a hexagonal closed packed, hcp, crystal structure. Critical resolved shear stresses, CRSS in single crystal Mg of a basal slip system at room temperature is approximately 1/100 those of non-basal slip systems on prismatic and pyramidal planes. Therefore, plastic deformation alloys should occur

almost entirely by basal slip. But the basal slip system provides only two independent slip systems, which is far fewer than the necessary five independent systems for homogeneous deformation. The additional independent slip systems can be provided through a complementary deformation by twinning, thus ensuring a homogenous deformation in hcp metals.

However, twinning is difficult with decreasing grain size and in [I.109 and 116] the ECAPed specimen with subsequent annealing exhibited a very high elongation to failure of 47% at room temperature. The grain size was measured to be 6.5 µm. The occurrence of non-basal slip was observed already at 2% of deformation. It was explained in terms of the yield anisotropy factor, which equals 100 but is reduced to 10, due to stress concentration aroused near grain boundaries and triple junctions for the grain structures usually smaller than 10 µm. And it is further reduced to a value of 1.1 due to grain-boundary compatibility stress [I.116]. As the deformation increased the twins were also found. Their role was twofold. From one side they are a source of work hardening, since their grain boundaries {10-12} act as a barriers for dislocation slip. From the other side they are a source of dynamic recovery, since some grain boundaries {10-11} may absorb dislocations by dissociating them and forming interface ledges. Therefore the activity of non-basal dislocation slip systems and the dynamic recovery were considered to be responsible for the large tensile ductility at room temperature of fine grained AZ31.

The yield anisotropy factor becomes lower with increasing temperature and non-basal slip occurs additionally to basal slip at elevated temperatures. Because of this fact the ECAP is usually performed at elevated temperatures to avoid cracking of the specimen. Nevertheless, twinning is also observed at elevated temperatures.

The ECAP processing temperature controlled the deformation mechanism at the initial stage of the deformation, thus different textures were developed from the same original material [I.115]. AZ31 alloy after extrusion with a typical fiber texture was subjected to 1 ECAP pass at 250 °C and 300 °C. At lower temperature the texture formation was dominated by tensile twinning and basal slip. While, at higher temperature, c+a slip predominated at the initial stage of the deformation. Subsequently, the crystals rotated by basal slip and grain boundary sliding during deformation for both specimens [I.115]. Finally, different textures were formed. The one formed at 250 °C, so-called shear texture, with basal planes aligned at an angle of 30-45° to the extrusion direction. And the other one formed at 300 °C with basal

planes parallel to the longitudinal direction, i.e. similar to the as-extruded texture.

Same situation was observed in [I.97], where the material after ECAP at low temperature exhibited the shear texture and the ECAP at high temperature resulted in identical to the as-extruded texture. The slip on the basal plane in the material with as-extruded textures would be difficult due to the low Schmidt factor and the strength increases with limited non-basal slip activities. As for the shear texture, where the basal planes are favorably oriented for shear during tensile test the yield stress is observed to be lower and ductility to be higher [I.96 and 102]. Since the grain size is normally reduced by ECAP to less than 10 μm, strengthening should be observed due to the Hall-Petch effect. But the softening effect due to texture anisotropy overwhelms the strengthening due to grain refinement through ECAP [I.96 and 97].

This statement could explain many contradictory results that were obtained after ECAP of Mg alloys, when compared to extruded specimens with coarser grains, ECAPed specimens exhibited lower yield strength and higher ductility. But it is well known, that ECAP does improve significantly mechanical properties [I.117] and very often strength and ductility simultaneously. In spite of a texture softening during ECAP there are some reports about the influence of grain boundary structure and dislocation distribution on the mechanical properties [I.33, 98 and 99]. Here both yield strength and elongations to failure were superior after ECAP processing than in as-received extruded state. Moreover, the "usual" effect of texture softening was observed at the specimen after ECAP at 225 °C with lower yield stress and higher ductility. But the more sophisticated ECAP processing with decreasing temperature from 225 to 180 °C for the last pass resulted in submicron grains and severely deformed microstructure, leading to improved properties [I.98]. It is apparent that the ECAP temperature plays the crucial role to obtain the "proper" microstructure for better properties.

So, as it can be seen from the preceding overview ECAP has a positive influence on the physical and mechanical properties of magnesium alloys. The great enhancement of the tensile strength [I.46 and 88] was achieved after ECAP. Furthermore, in [I.100 and 101] the ECAPed AZ31 alloy after forging was used as a knuckle arm and its tensile strength, fracture elongation and absorption energy were higher than those of T6-treated 6061 aluminum forging alloy specified by JIS. The statement about poor ductility of Mg alloys is turning into myth after ECAP processing. Elongations to failure at room temperature over 45% were reported in numerous works [I.102-

112], whereas 80% for AZ31 [I.110] and even 90% for Mg-Li alloy [I.38] were observed. Superplastic elongations at elevated temperatures were attained for the majority of studied alloys with the best values of 1780% for Mg-Li alloy [I.37], 1400% and 2040% for ZK61 [I.53 and 54].

But there are also some white spots and discrepancy in published results. The mechanical properties at elevated temperatures are barely studied. In Mg-Al-Zn group, for instance, there are good results in superplasticity for AZ61 [I.44, 69 and 70] and AZ91 [I.84], but poor for AZ31 [IV.7 and 9]. The effect of ECAP on hydrogen storage capacities was studied only on ZK61 [I.63] among magnesium alloys, though they may serve as an outstanding hydrogen storage medium due to their light weight, recyclability and improved physical properties after ECAP processing.

The aim of this work was to perform SPD via ECAP or HPT on new materials, which were not processed afore. To study their mechanical and physical properties at ambient and elevated temperatures, as well as microstructure before and after processing. To investigate the role of the ECAP temperature on the microstructure and mechanical properties of equally processed materials. To utilize this knowledge for optimizing the process parameters in order to achieve better results.

Literature:

[I.1]   R.Z. Valiev, Y. Estrin, Z. Horita, T.G. Langdon, M.J. Zechetbauer and Y.T. Zhu, JOM, 58_4 (2006) p. 33

[I.2]   R.Z. Valiev, Nature Mater., 3 (2004) p. 511

[I.3]   J.T. Wang, Mater. Sci. Forum, 503-504 (2006) p. 363

[I.4]   V.M. Segal, Russian Metall., 1 (1981) p. 99

[I.5]   V.M. Segal, Mater. Sci. and Eng., A271 (1999) p. 322

[I.6]   Y. Iwahashi, J. Wang, Z. Horita, M. Nemoto and T.G. Langdon, Scripta Mater., 35_2 (1996) p. 143

[I.7]   M. Furukawa, Z. Horita, M. Nemoto and T.G. Langdon, J. Mater. Sci., 36 (2001) p. 2835

[I.8]   R.Z. Valiev, R.K. Islamgaliev and I.V. Alexandrov, Progress in Materials Science 45 (2000) p. 103

[I.9]   R.Z. Valiev, "Nanosturkturye materialy, poluchennye intensivnoi plasticheskoi deformaciei", M.: Logos (2000) p. 272 (in russian)

[I.10]   V.M. Segal, Mater. Sci. Eng., A197 (1995) p. 157

[I.11]   M. Furukawa, Y. Iwahashi, Z. Horita, M. Nemoto and T.G. Langdon, Mater. Sci. Eng., A257 (1998) p. 328

[1.12]   K. Nakashima, Z. Horita, M. Nemoto and T.G. Langdon, Acta Mater., 46_5 (1998) p. 1589

[I.13]   V.M. Segal, "Processy plasticheskogo strukturoobrazovaniya metallov", Mn.: Navuka i Tehnika (1994) p. 232 (in russian)

[I.14]   A.P. Zhilyaev, G.V. Nurislamova, B.-K. Kim, M.D. Baró, J.A. Szpunar and T.G. Langdon, Acta Mater., 51_3 (2003) p. 753

[I.15]   A. Vorhauer, and R. Pippan, Scripta Mater., 51 (2004) p. 921

[I.16]   Y. Miyahara, N. Emi, K. Neishi, K. Nakamura, K. Kaneko, M. Nakagaki, Z. Horita, Mater. Sci. Forum, 503-504 (2006) p. 949

[I.17]   K. Matsubara, Y. Miyahara, Z. Horita and T.G. Langdon, Metallurgical and Materials Transactions, A35_6 (2004) p. 1735

[I.18]   A.-B. Ma, Y. Nishida, N. Saito, I. Shigematsu, S.-W. Lim, Materials Science and Technology, 19_12 (2003) p. 1642

[I.19]   A. Ma, S.W. Lim, Y. Nishida, M. Nagase, N. Saito, I. Shigematsu, A. Watazu, Mater. Sci. Forum, 426_4 (2003) p. 2735

[I.20]   Z.-H. Chen, Y.-Q. Cheng, W.-J. Xia, Materials and Manufacturing Processes, 22_1 (2007) p. 51

[I.21]   M.Y. Zheng, X.G. Qiao, S.W. Xu, K. Wu, S. Kamado, Y. Kojima, Mater. Sci. Forum, 475-479 (2005) p. 469

[I.22]   M.Y. Zheng, X.G. Qiao, S.W. Xu, K. Wu, S. Kamado and Y. Kojima, J. Mater. Sci., 40_9-10 (2005) p. 2587

[I.23]   M.Y. Zheng, X.G. Qiao, S.W. Xu, K. Wu, S. Kamado, Y. Kojima, Mater. Sci. Forum, 488-489 (2005) p. 589

[I.24]   M.Y. Zheng, S.W. Xu, X.G. Qiao, W.M. Gan, K. Wu, S. Kamado, Y. Kojima, H.G. Brokmeier, Mater. Sci. Forum, 503-504 (2006) p. 527

[I.25]   M. Yoshikawa, M. Kohzu, H. Watanabe, K. Higashi, Mater. Sci. Forum, 419-422 (2003) p. 769

[I.26]   H. Watanabe, T. Mukai, S. Kamado, Y. Kojima and K. Higashi, Mater. Trans., 44_4 (2003) p. 463

[I.27]   H. Watanabe, H. Somekawa, K. Higashi, J. Mater. Res., 20_1 (2005) p. 93

[I.28]   J. Čížek, I. Procházka, B. Smola, I. Stulíková, R. Kužel, Z. Matěj, V. Cherkaska, R.K. Islamgaliev, O.B. Kulyasova, Mater. Sci. Forum, 482 (2005) p. 183

[I.29]   J. Čížek, I. Procházka, B. Smola, I. Stulíková, R. Kužel, Z. Matěj, V. Cherkaska, R.K. Islamgaliev, O.B. Kulyasova, Mater. Sci. Forum, 503-504 (2006) p. 149

[I.30] J. Čížek, I. Procházka, B. Smola, I. Stulíková, R. Kužel, Z. Matěj, V. Cherkaska, R.K. Islamgaliev and O. Kulyasova, Acta Physica Polonica, A107_5 (2005) p. 738

[I.31] R. Kužel, Z. Matěj, V. Cherkaska, J. Pešička, J. Čížek, I. Procházka and R. K. Islamgaliev, J. Alloys and Compounds, 378_1-2 (2004) p. 242

[I.32] O.B. Kulyasova, R.K. Islamgaliev, A.R. Kil'mametov and R.Z. Valiev, Physics of Metals and Metallography, 101_6 (2006) p. 585

[I.33] R.Z. Valiev, N.A. Krasilnikov and N.K. Tsenev, Mater. Sci. Eng., A137 (1991) p. 35

[I.34] T.-C. Chang, J.-Y. Wang, C.-L. Chu and S. Lee, Mater. Lett., 60_27 (2006) p. 3272

[I.35] T. Liu, Y.D. Wang, S.D. Wu, R. Lin Peng, C.X. Huang, C.B. Jiang and S.X. Li, Scripta Mater., 51_11 (2004) p. 1057

[I.36] T. Liu, Y.D. Wang, S.D. Wu, S.X. Li, R.L. Peng, Y.B. Xu, Mater. Sci. Forum, 488-489 (2005) p. 177

[I.37] M. Furui, H. Kitamura, H. Anada and T.G. Langdon, Acta Mater., 55 (2007) p. 1083

[I.38] S. Kamado, T. Ashie, Y. Ohshima, Y. Kojima, Mater. Sci. Forum, 350_3 (2000) p. 55

[I.39] T. Liu, W. Zhang, S.D. Wu, C.B. Jiang, S.X. Li and Y.B. Xu, Mater. Sci. and Eng., A360_1-2 (2003) p. 345

[I.40] Y. Yoshida, L. Cisar, S. Kamado and Y. Kojima, Mater. Trans., 43_10 (2002) p. 2419

[I.41] J.–Y. Wang, T.-C. Chang, L.-Z. Chang and S. Lee, Mater. Trans., 47_4 (2006) p. 971

[I.42] Z. Horita, K. Matsubara, K. Makii and T.G. Langdon, Scripta Mater., 47_4 (2002) p. 255

[I.43] B.Q. Han and T.G. Langdon, Mater. Sci. and Eng., A410_Sp. Iss. SI (2005) p. 435

[I.44] Y. Miyahara, K. Matsubara, K. Neishi, Z. Horita, T.G. Langdon, Mater. Sci. Forum, 419_4 (2003) p. 551

[I.45] Y. Miyahara, K. Matsubara, Z. Horita, T.G. Langdon, Metallurgical and Mater. Trans., A36_7 (2005) p. 1705

[I.46] S. Kamado, T. Ashie, H. Yamada, K. Sanbun, Y. Kojima, Mater. Sci. Forum, 350_3 (2000) p. 65

[I.47] Z.W. Huang, Y. Yoshida, L. Cisar, S. Kamado, Y. Kojima, Mater. Sci. Forum, 419_4 (2003) p. 243

[I.48] Z.W. Huang, Y. Yoshida, S. Kamado, Y. Kojima, Mater. Sci. Forum, 488-489 (2005) p. 593

[I.49]   L. Lin, Z. Liu, L.J. Chen, T. Liu, S.D. Wu, Metals and Materials International, 10_6 (2004) p. 501

[I.50]   L. Yang, X.M. Yang, T. Liu, S.D. Wu, L.J. Chen, Mater. Sci. Forum, 488-489 (2005) p. 575

[I.51]   L. Lin, L.J. Chen, Z. Liu, Mater. Sci. Forum, 488-489 (2005) p. 581

[I.52]   L. Lin, W. Wu, L. Yang, L. Chen and Z. Liu, J. Mater. Sci., 41_2 (2006) p. 409

[I.53]   R. Lapovok, R. Cottam, P.F. Thomson, Y. Estrin, J. Mater. Res., 20_6 (2005) p. 1375

[I.54]   R. Lapovok, P.F. Thomson, R. Cottam and Y. Estrin, Mater. Sci. and Eng., A410_Sp. Iss. SI (2005) p. 390

[I.55]   R. Lapovok, P.F. Thomson, R. Cottam and Y. Estrin, J. Mater. Sci., 40_7 (2005) p. 1699

[I.56]   R. Lapovok, P.F. Thomson, R. Cottam and Y. Estrin, Mater. Trans., 45_7 (2004) p. 2192

[I.57]   T. Mukai, H. Watanabe and K. Higashi, Materials Science and Technology, 16_11-12 (2000) p. 1314

[I.58]   V.N. Chuvil'deev, T.G. Nieh, M.Yu. Gryaznov, A.N. Sysoev and V.I. Kopylov, Scripta Mater., 50_6 (2004) p. 861

[I.59]   V.N. Chuvil'deev, T.G. Nieh, M.Yu. Gryaznov, V.I. Kopylov and A.N. Sysoev, J. Alloys and Compounds, 378_1-2 (2004) p. 253

[I.60]   H. Watanabe, T. Mukai, K. Ishikawa, K. Higashi, Mater. Sci. Forum, 419_4 (2003) p. 557

[I.61]   H. Watanabe, T. Mukai, K. Ishikawa and K. Higashi, Scripta Mater., 46_12 (2002) p. 851

[I.62]   R.B. Figueiredo and T.G. Langdon, Mater. Sci. and Eng., A430_1-2 (2006) p. 151

[I.63]   V.M. Skripnyuk, E. Rabkin, Y. Estrin and R. Lapovok, Acta Mater., 52_2 (2004) p. 405

[I.64]   A. Galiyev and R. Kaibyshev, Mater. Trans., 42_7 (2001) p. 1190

[I.65]   B. Mingler, O.B. Kulyasova, R.K. Islamgaliev, G. Korb, H.P. Karnthaler and M.J. Zehetbauer, J. Mater. Sci., 42_5 (2007) p. 1477

[I.66]   O.B. Kulyasova, NanoSPD3 Conference, Fukuoka, Japan, September 22-26, 2005

[I.67]   A. Yamashita, Z. Horita and T.G. Langdon, Mater. Sci. and Eng., A300_1-2 (2001) p. 142

[I.68]   K. Matsubara, Y. Miyahara, K. Makii, Z. Horita, T.G. Langdon, Mater. Sci. Forum, 419_4 (2003) p. 497

[I.69]   Y. Miyahara, Z. Horita and T.G. Langdon, Mater. Sci. and Eng., A420_1-2 (2006) p. 240

[I.70]   Y. Yoshida, K. Arai, S. Itoh, S. Kamado and Y. Kojima, Mater. Trans., 45_8 (2004) p. 2537

[I.71]   S.Y. Chang, S.W. Lee, J.C. Kim, Y.S. Kim, D.H. Shin, Mater. Sci. Forum, 449_4 (2004) p. 645

[I.72]   S.-Y. Chang, S.-W. Lee, K.M. Kang, S. Kamado and Y. Kojima, Mater. Trans., 45_2 (2004) p. 488

[I.73]   Y. Yoshida, K. Arai, S. Itoh, S. Kamado and Y. Kojima, Science and Technology of Advanced Materials, 6_2 (2005) p. 185

[I.74]   W.J. Kim, H.G. Jeong, Mater. Sci. Forum, 419_4 (2003) p. 201

[I.75]   W.J. Kim, C.W. An, Y.S. Kim and S.I. Hong, Scripta Mater., 47_1 (2002) p. 39

[I.76]   W.J. Kim, S.I. Hong, Y.S. Kim, S.H. Min, H.T. Jeong and J.D. Lee, Acta Mater., 51_11 (2003) p. 3293

[I.77]   J. Gubicza, N.H. Nam, K. Máthis and V.V. Stolyarov, Zeitschrift für Kristallographie, Part 1 Suppl. 23 (2006) p. 93

[I.78]   K.N. Braszczynska–Malika and L. Froyen, Zeitschrift für Metallkunde, 96_8 (2005) p. 913

[I.79]   M. Greger, S. Rusz, M. Widomská, Key Eng. Mater., 274-276 (2004) p. 1083

[I.80]   X.S. Hu, K. Wu, M.Y. Zheng, S.W. Xu, Y.K. Zhang, Mater. Sci. Forum, 488-489 (2005) p. 737

[I.81]   K. Wu, X.S. Hu, M.Y. Zheng, Transactions of Nonferrous Metals Society of China, 15_Sp. Iss. 2 (2005) p. 276

[I.82]   M. Mabuchi, H. Iwasaki, K. Higashi, Mater. Sci. Forum, 243 (1997) p. 547

[I.83]   M. Mabuchi, M. Nakamura, K. Ameyama, H. Iwasaki, K. Higashi, Mater. Sci. Forum, 304_3 (1999) p. 67

[I.84]   M. Mabuchi, K. Ameyama, H. Iwasaki and K. Higashi, Acta Mater., 47_7 (1999) p. 2047

[I.85]   M. Mabuchi, Y. Chino, H. Iwasaki, T. Aizawa and K. Higashi, Mater. Trans., 42_7 (2001) p. 1182

[I.86]   Y. Chino and M. Mabuchi, Adv. Eng. Mater., 3_12 (2001) p. 981

[I.87]   A. Mussi, J.J. Blandin, L. Salvo and E.F. Rauch, Acta Mater., 54_14 (2006) p. 3801

[I.88]   J.J. Blandin, Mater. Sci. Forum, 426_4 (2003) p. 551

[I.89]   H. Somekawa and T. Mukai, Scripta Mater., 54_4 (2006) p. 633

[I.90]   H. Somekawa, A. Singh, T. Mukai, Phil. Mag. Lett., 86_3 (2006) p. 195

[I.91]   C.S. Chung, D.K. Chun and H:K: Kim, J. of Mech. Sci. and Techn., 19_7 (2005) p. 1441

[I.92]   H.-K. Kim, Y.-I. Lee and C.-S. Chung, Scripta Mater., 52_6 (2005)
         p. 473

[I.93]   H.K. Kim and W.J. Kim, Mater. Sci. and Eng., A385_1-2 (2004)
         p. 300

[I.94]   K. Xia, J.T. Wang, X. Wu, G. Chen and M. Gurvan, Mater. Sci. and
         Eng., A410_Sp. Iss. SI (2005) p. 324

[I.95]   J.Y. Wang, Y.H. Chen, Y.L. Yang, S. Lee, Mater. Sci. Forum, 488-
         489 (2005) p. 465

[I.96]   H.K. Kim, C.S. Chung, B.S. Cha, B.H. Goo and C.Y. Hyun,
         Praktische metallographie – Practical metallography, 41_3 (2004)
         p. 142

[I.97]   Y. Yoshida, L. Cisar, S. Kamado and Y. Kojima, Mater. Trans., 44_4
         (2003) p. 468

[I.98]   L. Jin, D.L. Lin, D.L. Mao, X.Q. Zeng, W.J. Ding, Mater. Sci. Forum,
         488-489 (2005) p. 601

[I.99]   L. Jin, D. Lin, D. Mao, X. Zeng and W. Ding, Mater. Lett., 59_18
         (2005) p. 2267

[I.100] L. Cisar, Y. Yoshida, S. Kamado, Y. Kojima and F. Watanabe, Mater.
         Trans., 44_4 (2003) p. 476

[I.101] L. Cisar, Y. Yoshida, S. Kamado, Y. Kojima, F. Watanabe, Mater.
         Sci. Forum, 419_4 (2003) p. 249

[I.102] S.R. Agnew, J.A. Horton, T.M. Lillo and D.W. Brown, Scripta Mater.,
         50 (2004) p. 377

[I.103] W.J. Kim and Y.K. Sa, Scripta Mater., 54_7 (2006) p. 1391

[I.104] Y. Li, D. Zhang, W. Chen, Y. Liu and G. Guo, J. Mater. Sci., 39_11
         (2004) p. 3759

[I.105] Y.Y. Li, Y. Liu, T.W.L. Ngai, D.T. Zhang, G.W. Guo, W.P. Chen,
         Transactions of Nonferrous Metals Society of China, 14_1 (2004)
         p. 53

[I.106] T. Mukai, H. Watanabe, K. Ishikawa, K. Higashi, Mater. Sci. Forum,
         419_4 (2003) p. 171

[I.107] T. Mukai, M. Yamanoi and K. Higashi, Mater. Trans., 42_12 (2001)
         p. 2652

[I.108] T. Mukai, M. Yamanoi, H. Watanabe and K. Higashi, Scripta Mater.,
         45_1 (2001) p. 89

[I.109] T. Kobayashi, J. Koike, T. Mukai, M. Suzuki, H. Watanabe, K.
         Maruyama, K. Higashi, Mater. Sci. Forum, 419_4 (2003) p. 231

[I.110] W.J. Kim and H.T. Jeong, Mater. Trans., 46_2 (2005) p. 251

[I.111] H.S. Kim, H.T. Jeong, H.G. Jeong, W.J. Kim, Mater. Sci. Forum, 475-
         479_Part 1-5 (2005) p. 549

[I.112] H.T. Jeong and W.J. Kim, Mater. Sci. Forum, 475-479_Part 1-5 (2005) p. 545

[I.113] L. Jin, D. Lin, D. Mao, X. Zeng, B. Chen and W. Ding, Mater. Sci. and Eng., A423_1-2_Sp. Iss. SI (2006) p. 247

[I.114] C.W. Su, L. Lu and M.O. Lai, Mater. Sci. and Eng., A434_1-2 (2006) p. 227

[I.115] Y. Yoshida, L. Cisar, S. Kamado, J. Koike, Y. Kojima, Mater. Sci. Forum, 419_4 (2003) p. 533

[I.116] J. Koike, T. Kobayashi, T. Mukai, H. Watanabe, M. Suzuki, K. Maruyama and K. Higashi, Acta Mater., 51_7 (2003) p. 2055

[I.117] Y. Estrin, Mater. Sci. Forum, 503-504 (2006) p. 91

[I.118] M. Furui, C. Xu, T. Aida, M. Inoue, H. Anada and T.G. Langdon, Mater. Sci. and Eng., A410_Sp. Iss. SI (2005) p. 439

II.   Different ECAP setups

<u>ECAP without back pressure</u>

The die has a 90° Φ angle and 0° Ψ angle so the equivalent strain obtained after each pass ε = 1.15, according to Iwahashi formula (I.1). The length of the entry channel allows pressing of the specimens up to 100 mm long. The cross-section of the channels is square, 10x10 mm^2. The die is made of the X38CrMoV51 steel that was quenched and additionally age-hardened. The exit channel was made to be shorter to avoid unnecessary friction in the channel, thus keeping the pressing force low. The die itself is placed in the Instron ram with the movable under part, Fig. II.1. It can be heated up to 300-350 °C with the heating pistons located inside the die. To prevent overheating of the hydraulic oil or the load cell of the machine there are two cooling units, which are connected to the water.
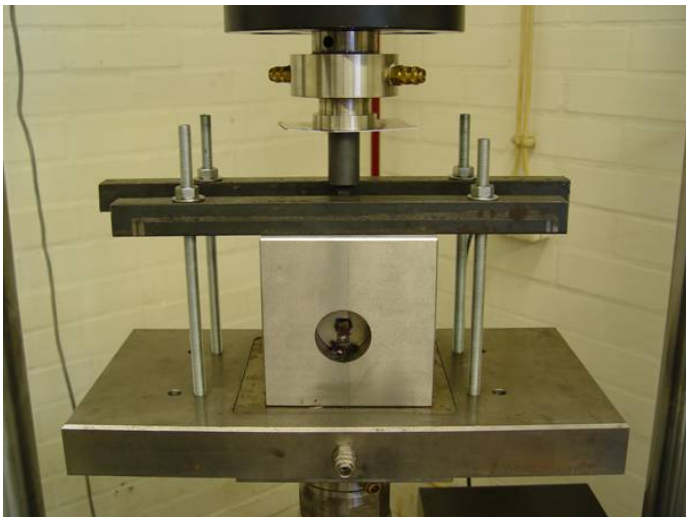
Fig. II.1 ECAP rig in Institute for Material Science, TU Clausthal, Germany

The die consists of two halves, which are linked using 10-15 screws. So, the specimen is getting greased with MoS_2 lubricant for better processing and put inside the entry channel. The plunger is also treated with MoS_2 lubricant and is then inserted in the entry channel. The processing speed and temperature are automatically controlled. After the pressing is finished, the plunger is usually extracted with low

force and after cleaning is ready for the next pass. Another specimen is greased and inserted again, thus pushing out the first one. At the same time, the first specimen serves as a kind of back pressure, creating small amount of a hydrostatic pressure. So, it takes approximately 20 to 30 minutes before the specimen is extracted from the die and chilled down to the room temperature. After each pressing the specimens are usually bigger in their size due to the elastic spring back effect, so they have to be grinded down to 10x10 mm^2 or they would not match in the entry channel. With the proceeding processing the length of the specimens therefore becomes smaller and even the specimen with the initial length 100 mm can be used only for the one small tensile test specimen at the end.

ECAP with back pressure

This die consists also of two halves. But together they form round geometry, which is pressed in the cylindrical metal jacket, Fig. II.2. There are four holes in the jacket for the electrical heaters. Further, this jacket with the die is placed in the rig, where two plungers are put into the channels. The main plunger is set from the top in the entry channel and the second plunger, which is responsible for the back pressure locates in the exit channel. The second hydraulic cylinder creates a pressure on the second plunger, the temperature is raised up to the given one and the pressing can start. This ECAP rig was installed in the old, but powerful press, so the speed was controlled manually.

Fig. II.2 ECAP rig at Monash University, Melbourne, Australia

After the pressing of the 35 mm long billets the die was pressed out of the jacket and the billet was extracted and quenched. Hence, the time the billet spent at the working temperature was very short, around 5 minutes, which provided a very favorable effect on the microstructure forming. The processed billets were also bigger in their dimensions and since they had a round geometry, they were machined back to 10 mm in diameter after each pass. As a result, the length of the billets after 6 passes did not exceed 30 mm.

III. Mechanical properties of thermally aged Mg-Sm and Mg-Al-Ca alloys at ambient and elevated temperatures after SPD via ECAP and HPT

III.1. Introduction

Magnesium alloys with rare earth elements (RE) processed via ECAP or HPT were barely studied (see Ch. I). There are some reports describing Mg-10%wtGd [I.8-11 and 12] deformed by HPT. However, there is no information about the age-hardening behavior of the alloy. The system Mg-Sm and Mg-Al-Ca were not investigated at all, though they have a great potential to be used in the automotive parts, due to their high mechanical properties at ambient and elevated temperatures.

The Mg-Sm alloys introduce a perspective alloy system characterized by high strength at room and elevated temperatures. The properties of the alloys to a great extent are determined by the high strengthening during the decomposition of supersaturated magnesium solid solution. The preliminary investigations of the Mg-Sm alloys were performed in the works [III.2-3], which are related to this work. In these papers the joint effect of SPD and solid solution decomposition on strength properties was studied and it is further investigated with following transition from SPD via HPT to SPD via ECAP.

III.2. Initial material and its processing prior to SPD

Mg-Al-Ca

HPT

The Mg-Al-Ca alloy was in as-cast condition before SPD via HPT. The alloy has 0.62wt% of Al and 0.57wt% of Ca. One part of the as-cast initial material was quenched from 475 °C and the other one was prepared for HPT. Samples in as-cast, quenched and HPT condition were aged and the kinetics of aging through microhardness and specific electrical resistance measurements was observed. The aging temperature was chosen 175 °C for the maximum effect of strengthening at this temperature [III.4-5].

ECAP

The initial alloy for ECAP had a similar composition obtained by chemical analysis. 0.49wt% of Al and 0.47wt% of Ca were detected in the alloy. So, from here the alloy will be designated as Mg-Al-Ca, since the chemical composition is very close. The initial as-cast material was divided into three main groups to investigate their mechanical properties and microstructure within a group and for the illustrative comparison between the groups after different thermomechanical treatments:

- First group – as-cast condition after different heat treatments

  - Homogenization at 475 °C for 4 hours with cooling in the air – "annealed"

  - Homogenization at 475 °C for 4 hours with subsequent quenching in water – "quenched"

  - Homogenization at 475 °C for 4 hours with cooling in the air and subsequent aging at 175 °C for 4 hours – "aged"

  - Homogenization at 475 °C for 4 hours with subsequent quenching in water followed by aging at 175 °C for 4 hours – "quenched and aged"

- Second group – the „annealed" material after extrusion with and without subsequent aging

  - Homogenization at 415 °C for 8 hours with cooling in the air and following extrusion at 340 °C – "extruded"

  - Homogenization at 415 °C for 8 hours with cooling in the air and following extrusion at 340 °C with subsequent aging at 175 °C for 4 hours – "extruded and aged"

- Third group – ECAP of different states

  - Homogenization at 475 °C for 4 hours with cooling in the air and following ECAP at 300 °C – "ECAP"

  - Homogenization at 475 °C for 4 hours with subsequent quenching in water and following ECAP at 300 °C – "quenched and ECAPed"

  - Homogenization at 415 °C for 8 hours with cooling in the air, subsequent extrusion at 340 °C and following ECAP at 300 °C – "extruded and ECAPed"

- Homogenization at 415 °C for 8 hours with cooling in the air and following ECAP at 220 °C with back pressure – "ECAP with BP"

Homogenization at 475 °C was performed under protective atmosphere of argon and at 475 °C in alumina oxide, Al_2O_3. These precautions were made to avoid extensive oxidization or ignition of the material. The extrusion was carried out at 340 °C with the diameter reduction from 70 to 16 mm, so the ratio was approximately 1:4.4. The extrusion speed was 1 mm/s. The extruded rod was straight and exhibited a good surface over the whole length without any cracks or inhomogeneities. This rod was used to prepare samples for ECAP processing or the extruded material was directly studied by microhardness or in tensile tests. After ECAP some specimens were additionally aged at 175 °C for 4 hours to investigate the effect of age hardening on mechanical properties. Such specimens will be designated accordingly by adding of the ending "aged" to the related description.

Mg-Sm

HPT

The alloy with 4.5wt% of Sm was obtained by melting in electrical resistance furnace. The melts were poured into steel mould with three round cavities. Small ingots of 15 mm in diameter and of about 90 mm in length were casted. The ingots were cut into cylindrical pieces which were solution treated at 510 °C for 5 hours and quenched in cold water. After quenching, the pieces were aged at 200 °C for 8 hours and at 300 °C for 6 hours. The aging at 200 °C, 8 hours corresponded to maximum strengthening during Mg solid solution decomposition and the aging at 300 °C, 6 hours corresponded to actually full Mg solid solution decomposition and softening [III.1]. Then the samples were subjected to SPD by HPT. Further, the specimens before and after SPD were studied by specific electrical resistance and microhardness measurements during aging at 200 °C.

ECAP

Chemical analysis of the studied alloy showed the presence of 3.81wt% of Sm. The homogenization after casting was carried out at 490 °C for 8 hours under protective argon atmosphere with cooling in the air. Further, the ingot was extruded at 400 °C with the change in diameter from 70 to 16 mm, i.e. with ratio 1:4.4. The extrusion speed was 1 mm/s. After this preliminary processing the material was also divided into groups as it was done with Mg-Al-Ca. Since there was no

cast material left for investigations, the division starts from the second group – after extrusion.

- Second group – extruded material with or without aging

    – Homogenization at 490 °C for 8 hours with cooling in the air and following extrusion at 400 °C – "extruded"

    – Homogenization at 490 °C for 8 hours with cooling in the air, following extrusion at 400 °C and subsequent aging at 200 °C for 4 hours – "extruded and aged"

- Third group – ECAP of different states

    – Homogenization at 490 °C for 8 hours with cooling in the air, following extrusion at 400 °C and subsequent ECAP at 300 °C – "extruded and ECAPed"

    – Homogenization at 490 °C for 8 hours with cooling in the air, following extrusion at 400 °C and subsequent ECAP at 220 °C with back pressure – "ECAP with BP"

The argon gas in this case was also used as a protection against oxidization or ignition. The extrusion itself, strictly speaking, was performed on the cone shaped ingot. From one side the diameter was 65 mm and on the other side – 45-50 mm with a relatively big bubble. Because of this the ingot was firstly undergone to setting and then extruded. The surface of the rod was very rough, with many cross skin-deep cracks. A lot of lengthwise grooves over the whole length of the rod were observed. The rod was bent and not everywhere of the round cross-section. The ECAP specimens were prepared from the rod.

III.3. SPD of Mg-Al-Ca and Mg-Sm alloys

Mg-Al-Ca

The HPT processing of Mg-Al-Ca alloy was carried out in as-cast state. The samples were subjected to SPD at room temperature by torsion under pressure of 4 GPa to $\varepsilon \approx 6$, which means that 5 revolutions were made.

ECAP of this alloy without back pressure was performed at 300 °C up to 6 passes using route B_C and pressing speed of 10 mm/min. The billets for ECAP were cut from the as-cast and extruded material with

dimensions 10x10x100 mm^3. The relatively high temperature of 300 °C was chosen due to the poor deformability of the alloy, especially of its cast state. Among different cast condition the most problems occurred with the billets after quenching, so in the "quenched" condition. From the several billets prepared for ECAP it was possible to press only few of them to 6 passes. And they also exhibited some amount of cracks. The ECAP of the "extruded" state was very successful due to finer grain after preliminary extrusion.

ECAP of the "annealed" condition was carried out using a rig with an additional hydraulic cylinder, thus providing a controllable back pressure. The billets prepared for ECAP were 10 mm in diameter and 35 mm in length. For Mg-Al-Ca alloy the force of the back pressure was as high as 131 MPa for each pass. Owing to the presence of back pressure it was possible not only to press easily the material up to 6 passes, but also to reduce temperature down to 220 °C.

Mg-Sm

HPT was applied to the specimens that were preliminary quenched, quenched and aged at 200 °C or 300 °C. The SPD was performed at room temperature and 200 °C under a pressure of 4 GPa up to 5 revolutions, which corresponds to the equivalent strain of ~6.

At the processing temperature of 300 °C the ECAP of the "extruded" was not successful. Firstly, the dimensions of the billets for ECAP were supposed to be 10x10x100 mm^3, but because of the different cross-section of the extruded rod which was somewhere less than 16 mm or even of ellipse form, the billets had rounded corners. Secondly, already after the first pass the billets split in longitudinal direction which is very untypical for cracking during ECAP. The reason seems to be in the grooves that were obtained after extrusion. Nevertheless the billets were ECAPed to full 6 passes in order to study microstructure, microhardness and other important properties.

The ECAP processing with back pressure of the "extruded" state was carried out on the billets having 10 mm in diameter and 35 mm in length. The force of the back pressure was increase up to 218 MPa, thus hindering initiation and propagation of the cracks on the internal defects obtained during extrusion. The ECAP resulted in achieving of 6 passes at the decreased temperature of 220 °C.

III.4. Evolution of the microstructure during SPD via ECAP

Mg-Al-Ca

The optical microscopy was used to study the microstructure of the Mg-Al-Ca alloy in the initial state, after different heat treatments and then after extrusion or subsequent ECAP processing.
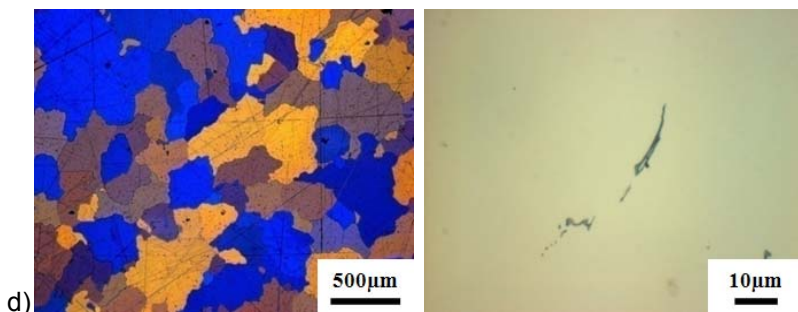
d)
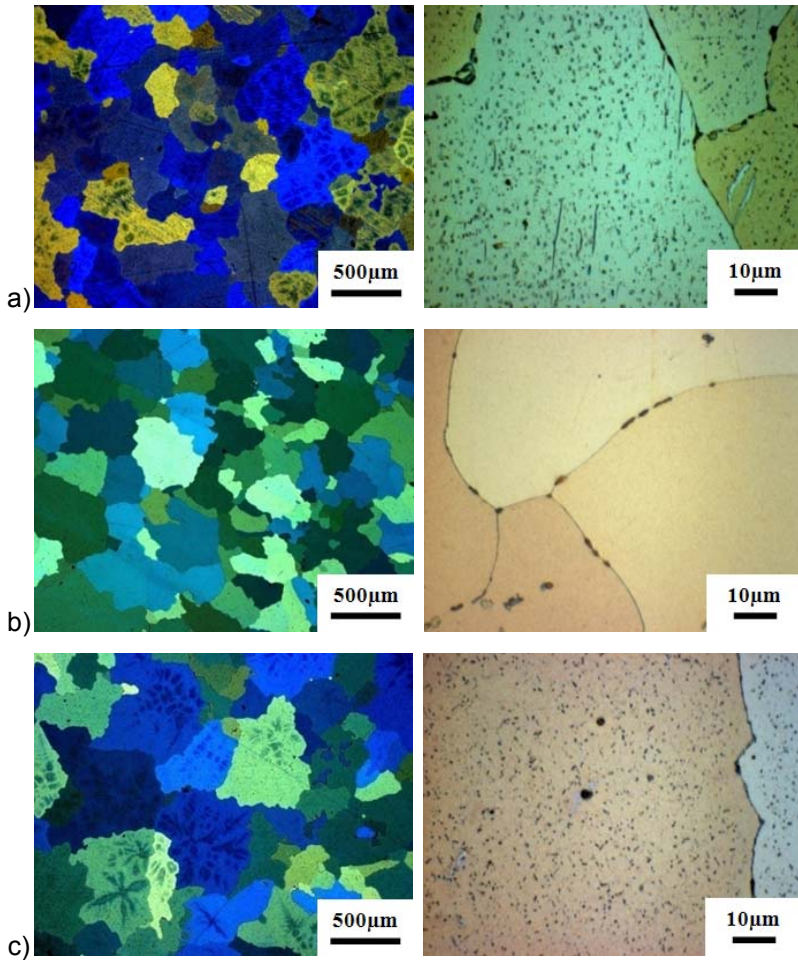
Fig. III.1 Microstructure of the Mg-Al-Ca alloy in a) „annealed", b) „quenched", c) „aged" and d) „quenched and aged" conditions. The images on the left were taken in polarized light, on the right in normal light. d) on the right shows an unetched sample

The images of the first group of the material in different cast conditions are presented in Fig. III.1. The mean grain size of each condition is very similar and can be estimated 420 µm. The polarized light at a low magnification was specially used to highlight the grain contours. One interesting feature became visible in polarized light, that the grains in "annealed" and "aged" conditions contained flowers-like forms inside indicating the dendrite substructure after casting, Fig. III.1 a) and c). Whereas such "flowers" became more clear after aging even by normal light. After quenching however, they were dissolved in the matrix and did not appear even after subsequent aging, Fig. III.1 b) and d).

The right row of the images in Fig. III.1 shows the microstructure at higher magnification, where precipitates, their form and distribution are clearly visible. In all states there is a presence of big particles that were not dissolved during the solution heat treatment.

These particles are aluminum and calcium rich and have a composition Al_2Ca according to [III.4]. Their preferable position is in the grain boundaries but also numerous particles are observed inside the grains. The specimens "annealed" and "aged" exhibit similarly big amount of precipitates and their distribution. In the "quenched" condition the grains are almost free from precipitates, which segregate in a very disperse form after additional aging. On the Fig. III.1 d) the "quenched and aged" state in unetched condition is shown. It is a typical photo for each state, where bigger particles in a needle shape are visible at higher magnification. The form of the particles is very different – smaller particles have usually a rounded shape.
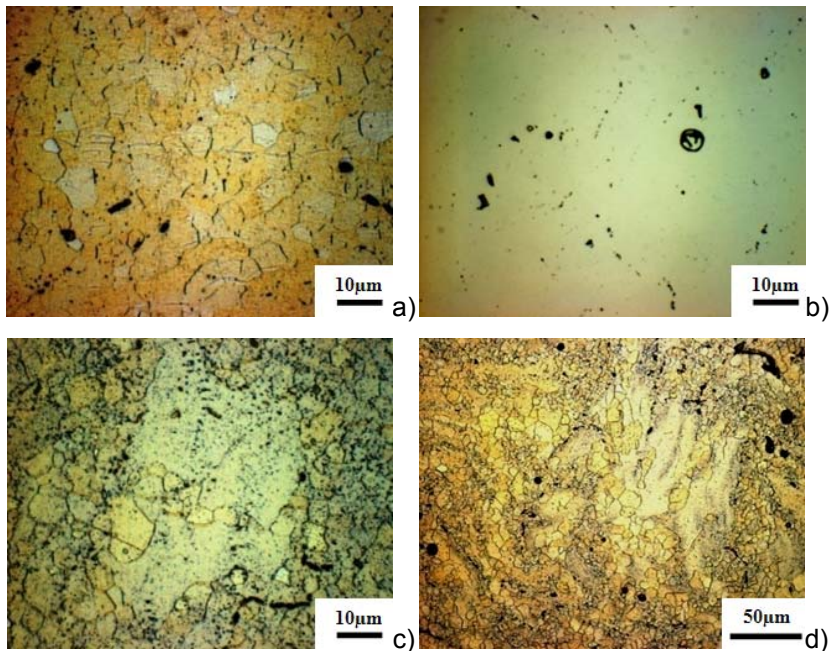
45

Fig. III.2 Microstructure of the Mg-Al-Ca alloy in a) "extruded" and b)-d) "extruded and aged" conditions. b) shows an unetched sample

After the extrusion the grain size is drastically reduced, Fig. III.2. The "extruded" sample exhibit equiaxed and homogeneous grains with the grain size ~9 μm, Fig. III.2 a). A certain amount of twins is also observed.

During the following aging an abnormal grain growth is occurred. There are areas with small grains, <10 μm and large grains that can reach up to 100 μm in some directions, Fig. III.2 c) and d). The bigger amount of dispersed precipitates is existent in the "extruded and aged" sample. For both states the presence of impurities or their agglomerations on the small area in the sample is usual. Precipitates have different shapes and often hollow round particles with included α-Mg matrix can be observed, Fig. III.2 b).
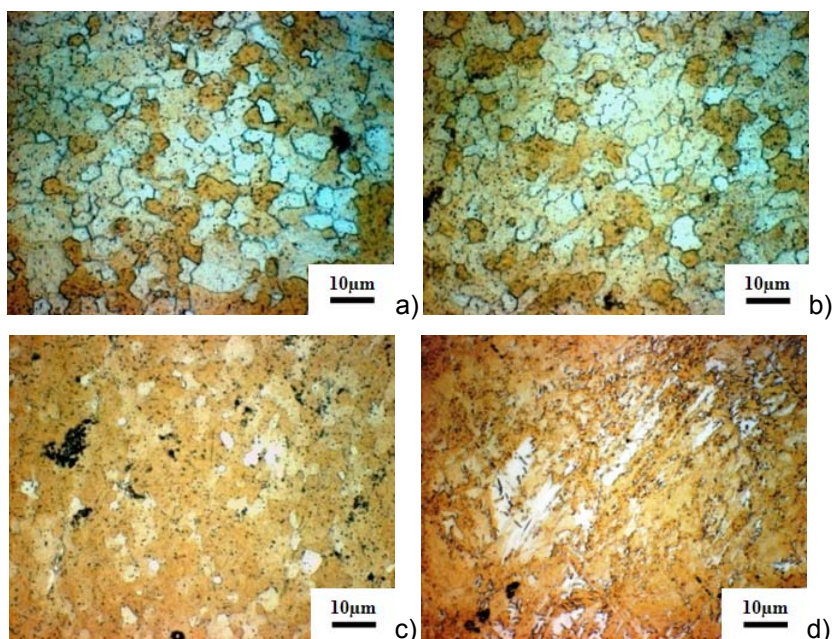
Fig. III.3 Microstructure of Mg-Al-Ca alloy in a) "ECAP", b) "quenched and ECAPed", c) "extruded and ECAPed" and d) "ECAP with BP"

The grain size is further reduced due to ECAP processing. Microstructures of "ECAP", "quenched and ECAPed" and "extruded and ECAPed" are very similar and exhibit a grain size 1-3 μm, Fig. III.3 a)-c). The sample processed by ECAP with back pressure at a low temperature of 220 °C has a very deformed microstructure, Fig. III.3 c), so the transmission electron microscopy (TEM) investigation was necessary to measure the grain size.

On the TEM images shown in Fig. III.4 the difference between ECAP at high (300 °C) and low (220 °C) is clearly visible. The mean grain size after ECAP at high temperature is 1-3 μm, as it was already asserted in optical microscopy, Fig. III.3. And it is much smaller after ECAP at 220 °C. The mean grain size was measured to be around 500 nm, Fig. III.4 c) and d). But not only the grain size was changed with the change of the ECAP temperature. In comparison with the equiaxed grains in the "ECAP" sample, the microstructure in "ECAP with BP" is severely deformed, exhibits high density of dislocations and ill-defined grain boundaries.
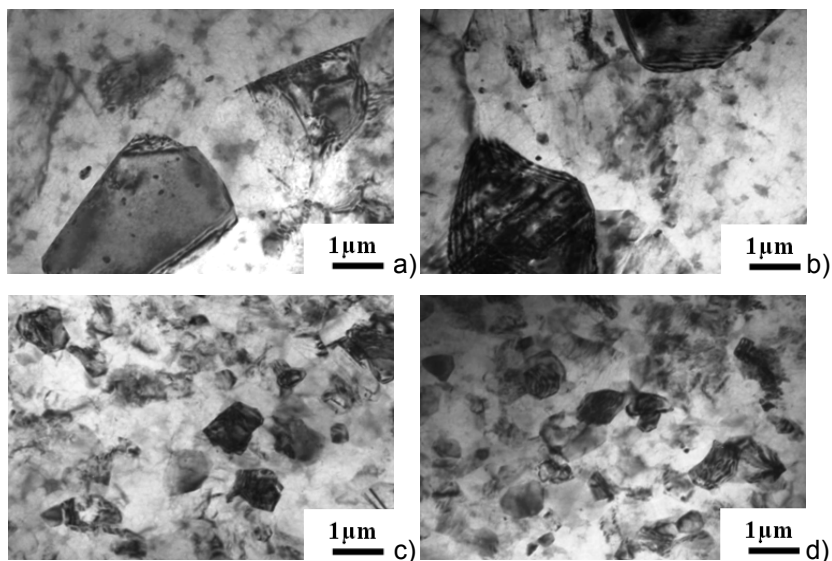
Fig. III.4 Microstructure of Mg-Al-Ca alloy after ECAP at 300 °C in "ECAP" condition – a), b) and at 220 °C in "ECAP with BP" condition – c), d)

<u>Mg-Sm</u>

In the "extruded" condition the grains from 5 to 30 µm were observed, with the average grain size of 15 µm, Fig. III.5 a). Deformation twins are clearly visible. Big precipitates are distributed homogeneously, but the small ones are segregated in large amounts in some areas, and almost nothing in other areas of the sample. The precipitations are samarium rich and have a composition $Mg_{41}Sm_5$ according to the Mg-Sm phase diagram [III.1]. After the subsequent aging the range of grain sizes became narrow, however the mean grain size was slightly increased up to 20 µm. The distribution of precipitates persisted the same and the twins after extrusion are still visible, Fig. III.5 b).

After ECAP the grain size was reduced in the similar way as for the Mg-Al-Ca alloy, i.e. down to approximately 3 µm. The grains are homogeneous and equiaxed, Fig. III.5 c). After the ECAP processing with back pressure was applied on Mg-3.8wt%Sm at 220 °C the microstructure observed in optical microscopy became severely deformed, Fig. III.5 d). Since it was impossible to resolve any structural components in the "ECAP with BP" sample by means of metallographic method, the TEM investigations were performed. They

were carried out on the "extruded and ECAPed" and "ECAP with BP" conditions to compare the obtained microstructure, Fig. III.6.
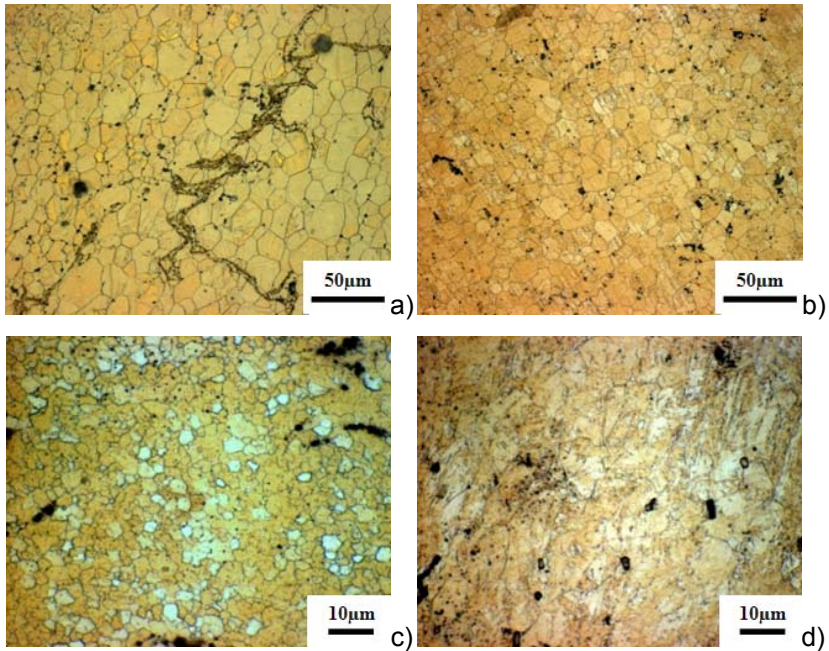

Fig. III.5 Microstructure of Mg-3.8wt%Sm alloy in a) "extruded", b) "extruded and aged", c) "ECAP" and d) "ECAP with BP" condition

The TEM images of Mg-3.8wt%Sm in Fig. III.6 a) and b) show a good accordance to the average grain size obtained in optical microscopy. The mean grain size was measured to be about 3 µm as well. The grains are equiaxed and the grain boundaries are in equilibrium state. The dislocation density is not so high and is comparable with Mg-Al-Ca alloy after ECAP at 300 °C. The precipitates can be well observed inside the grain structure and in the grain boundaries, Fig. III.6 a).

The microstructure changes dramatically with decreasing of the ECAP temperature down to 220 °C. Severely deformed zones with sub-grains are observed after 6 passes at lower temperature, Fig. III.6 c) and d). The dislocation density is very high and grain boundaries are contained in non-equilibrium state. The grain size differs from 100 to 600 nm with the average value of 300 nm, which is less than by Mg-Al-Ca alloy processed by similar conditions.
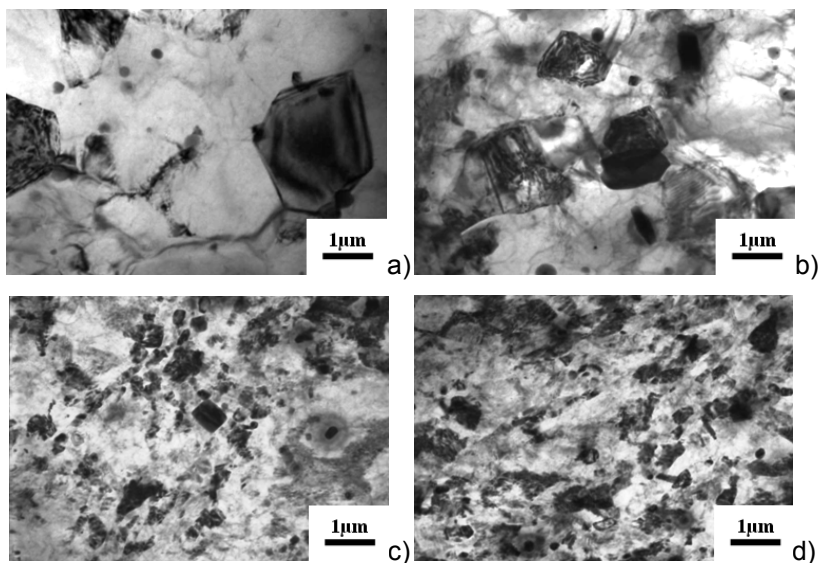
Fig. III.6 Microstructure of Mg-3.8wt%Sm alloy after ECAP at 300 °C
in "extruded and ECAP" condition – a), b) and at 220 °C in "ECAP with
BP" condition – c), d)

III.5.   Mechanical properties obtained in different conditions

Mg-Al-Ca

HPT

The drop in the value of the specific electrical resistivity with the aging
time corresponds to the decomposition of the supersaturated Mg
based solution rich with alloying elements. The investigations
performed during the aging processing of Mg-Al-Ca alloy have
indicated the change in specific electrical resistivity with the
segregation of Al_2Ca phase [III.4].
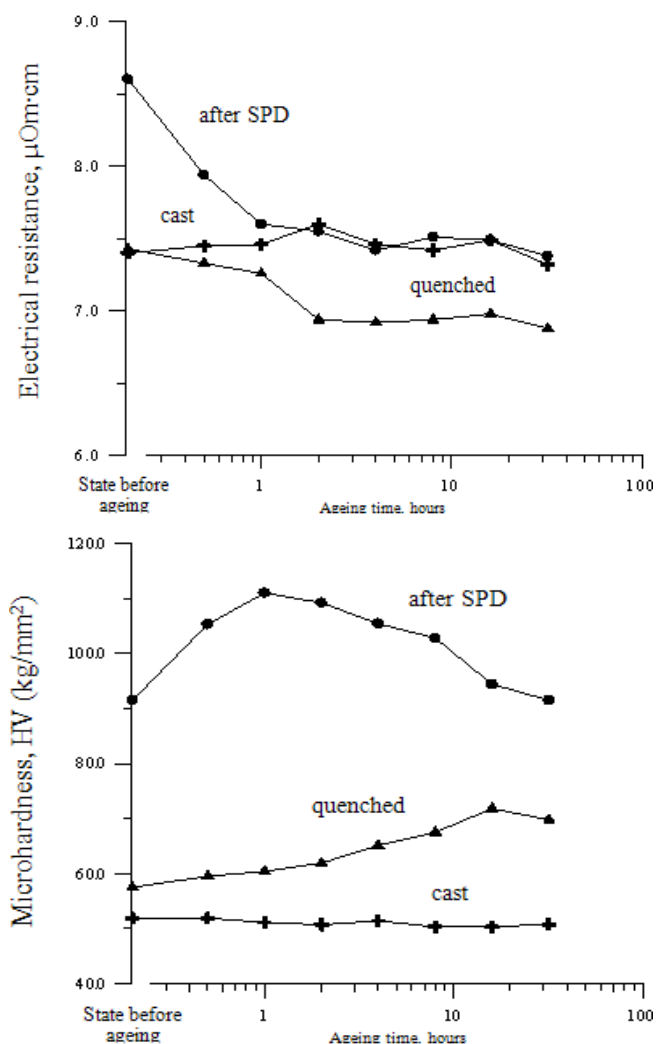
Fig. III.7 Specific electrical resistance (top) and microhardness (bottom) of the Mg-Al-Ca alloy vs. aging time at 175 °C

From Fig. III.7 it is apparent that the samples after HPT and after quenching exhibit a decrease in the specific electrical resistivity due to the depletion of Mg solid solution by Al_2Ca. The degree of the change in the specific electrical resistivity is much higher for the sample processed via HPT and the initial value as well. The behavior of the

curves measured for specific electrical resistance correlates well with the curves obtained from microhardness measurements.

The decomposition of the supersaturated solution results in the enriching of the α-Mg matrix with hard and stable precipitates of the second phase. Due to this fact the precipitation hardening takes place and the degree of the precipitation reflects in the level of strengthening. The maximum strength is observed after HPT processing and subsequent aging at 175 °C for short time. The kinetics of the aging for the quenched material is much lower, so it is necessary to hold the sample for a longer time until the maximum strengthening due to the full decomposition of the solid solution at a given aging temperature will be achieved. The sample in the as-cast state does not exhibit any significant change in the specific electrical resistance and as a consequence, no strengthening or softening is observed during aging.

ECAP

Tensile tests were carried out at initial strain rate of 1×10^{-3} s^{-1} using the samples with initial gauge length of 17 and 12.5 mm. The smaller gauge length was chosen for the samples after ECAP processing, due to the smaller size of the billets after 6 passes. To compare the influence of the specimen's geometry tensile tests were first performed on the as-cast and extruded materials using both geometries. These tests resulted in the excellent match of the strength properties and some higher elongations to failure were obtained by shorter specimens.

Since the effect of the aging on the Mg-Al-Ca was investigated after SPD via HPT the optimum temperature was also used for the samples after ECAP and extrusion. Because of that fact that the specimens were bigger, the time was increased from 1 hour to 4 hours compared with tiny samples studied after HPT.

The strengthening effect on the yield stress due to aging is obvious at room temperature, Fig. III.8. Quenching of the cast sample increased the yield stress from 82 MPa to 121 MPa, but the additional aging contributed to the further enhancement of the yield stress up to 162 MPa for "quenched and aged" state.
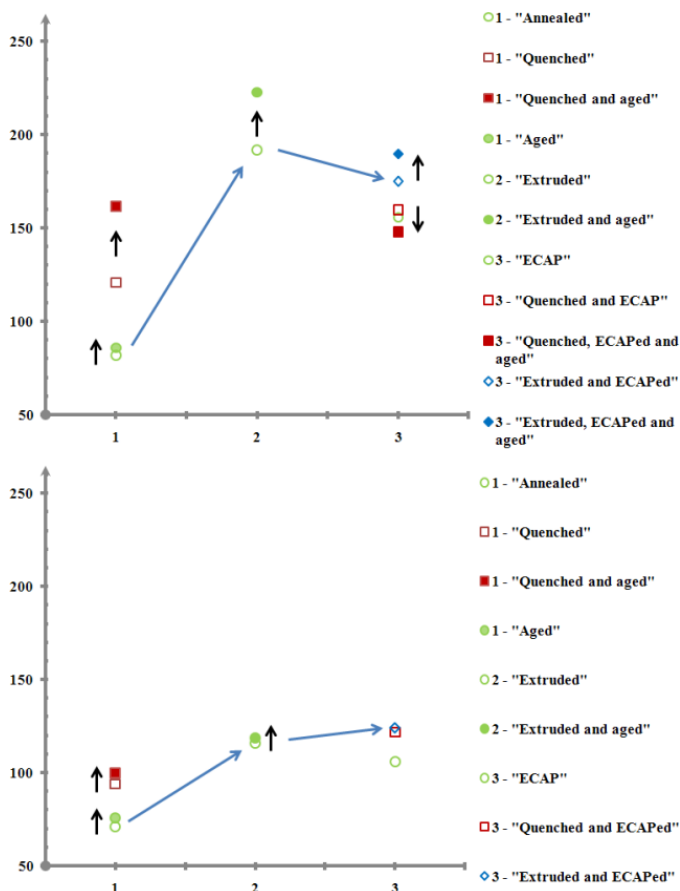
Fig. III.8 Influence of the thermomechanical treatments on the yield stress (MPa) at room temperature (top) and at 160 °C (bottom). On the X axis different groups are shown: 1 – cast, 2 – extruded and 3 – ECAPed conditions

The following extrusion of the "annealed" state led to the increased value of the yield stress and after the subsequent aging the yield stress was further improved up to 223 MPa in "extruded and aged" state. This value is the maximum one obtained for the Mg-Al-Ca in this work. The adding of ECAP processing slightly lowers the yield stress, which was improved again after the subsequent aging up to 190 MPa in "extruded, ECAPed and aged" state. Direct ECAP of the cast material increased yield strength up to 160 MPa, though it was decreased down to 148 MPa after the additional aging.

Tensile test at elevated temperature resulted in overall drop of the yield stress. The observed tendency of the improving of the yield stress is persisted, though the level of the improvement is considerable smaller. The "extruded and ECAPed" sample exhibited the highest value of 124 MPa. Thus the most softening is occurred in the "extruded and aged" condition, where the yield stress at room temperature has drop from 223 MPa to 119 MPa at 160 °C. The value of the yield stress of the cast material directly after ECAP is of the same order as of the cast material itself in "quenched and aged" state, i.e. 106 MPa and 100 MPa, respectively.
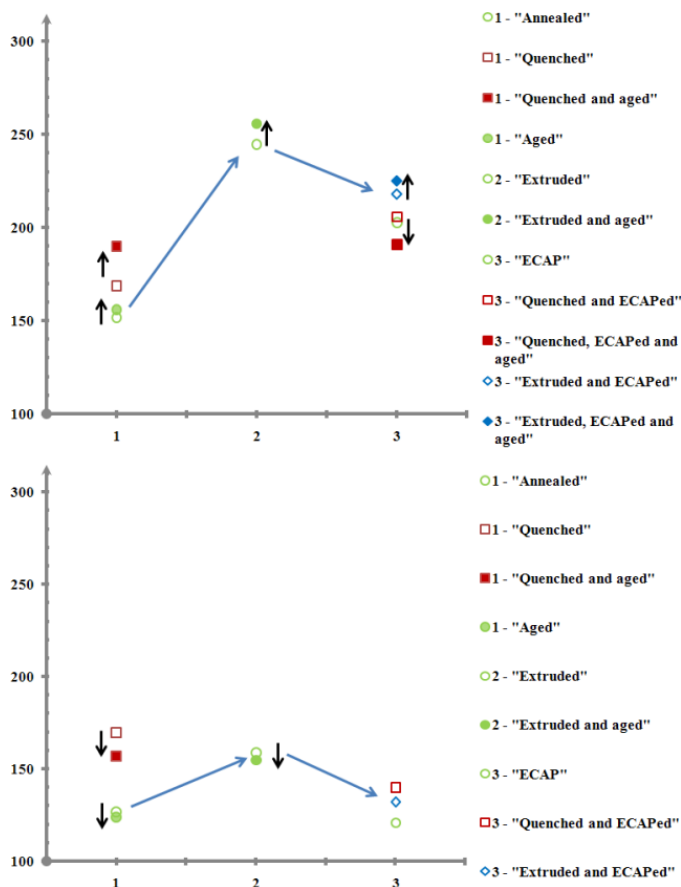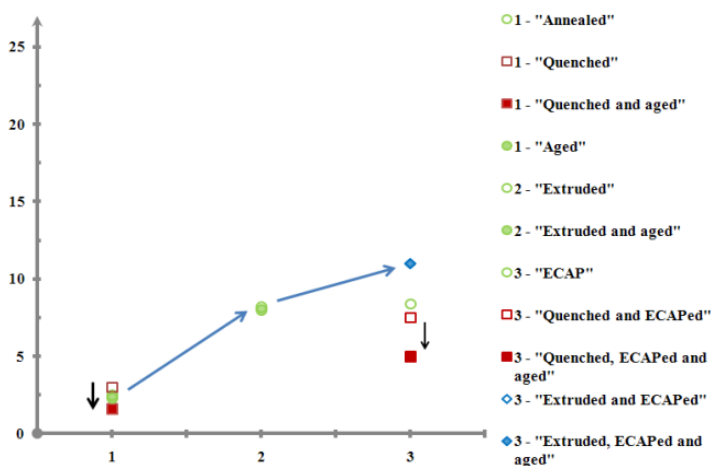

Fig. III.9 Influence of the thermomechanical treatments on the ultimate tensile stress (MPa) at room temperature (top) and at 160 °C (bottom). On the X axis different groups are shown: 1 – cast, 2 – extruded and 3 – ECAPed conditions

The ultimate tensile stress changes in the similar way as the yield stress after different thermomechanical treatments, Fig. III.9. The positive effect of the aging on the tensile strength was observed almost for all states at room temperature. The highest value of the tensile strength among the cast samples has still "quenched and aged" sample, 190 MPa. The highest value of the tensile strength among all the states was observed by the "extruded and aged" sample, 256 MPa. The ECAP processing of the extruded material with subsequent aging resulted only in 225 MPa – "extruded, ECAPed and aged" state. ECAP performed directly on the cast sample did not show any significant improvement in the tensile strength. Moreover, the "quenched, ECAPed and aged" sample exhibited only 191 MPa, which is equal to the tensile strength obtained for the "quenched and aged" cast sample.

At the elevated temperature the interesting fact is observed, the ultimate tensile stress of the "quenched" cast condition is the highest value among all the states and is equal to 169 MPa, which is higher than after extrusion – 159 MPa ("extruded") or after ECAP – 140 MPa ("quenched and ECAPed"). The additional aging almost did not exert any significant change of the tensile strength, even providing some softening for all states.

In Fig. III.10 the positive effect of ECAP processing on the ductility of Mg-Al-Ca is clearly visible. For both room and elevated temperature the additional aging did not provide any consequent result. Sometimes it was beneficial to age a sample regarding the elongation to failure, sometimes the effect was rather negative and, for example, for the "extruded" material there was no alternation at all.
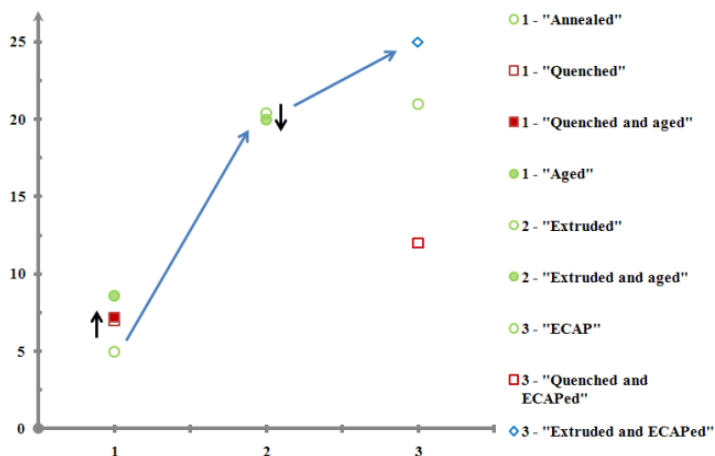
Fig. III.10 Influence of the thermomechanical treatments on the elongation to failure (%) at room temperature (top) and at 160 °C (bottom). On the X axis different groups are shown: 1 – cast, 2 – extruded and 3 – ECAPed conditions

The cast material has a very low ductility at room temperature of about 2-5%. After extrusion it is increased up to 8% and further increased up to 11% due to subsequent ECAP. The ECAP of the cast samples directly resulted in lower ductility.

At elevated temperature the overall improvement of ductility is observed. The most improvement is attained by the "extruded and ECAPed" sample from the 11% at room temperature up to 25% at 160 °C. After the extrusion the elongation to failure reached 20%. The ECAP of the cast material without preliminary extrusion allowed to increase the ductility up to 21%, but this is still inferior to the ductility of the "extruded and ECAPed" state.

The microhardness measurements were performed for all states, Fig. III.11. At room temperature the highest value is observed for the "quenched and aged" sample for the cast material. The samples after extrusion and ECAP exhibited almost the same value of the microhardness. This value of the deformed states was higher than of the "annealed" sample and only slightly higher than of the "aged" or "quenched" condition. Moreover it was inferior to the "quenched and aged" condition, due to the high level of solid solution decomposition. The highest microhardness however was obtained by "ECAP with BP" sample, which microhardness was significantly enhanced after the ECAP processing at lower temperature.
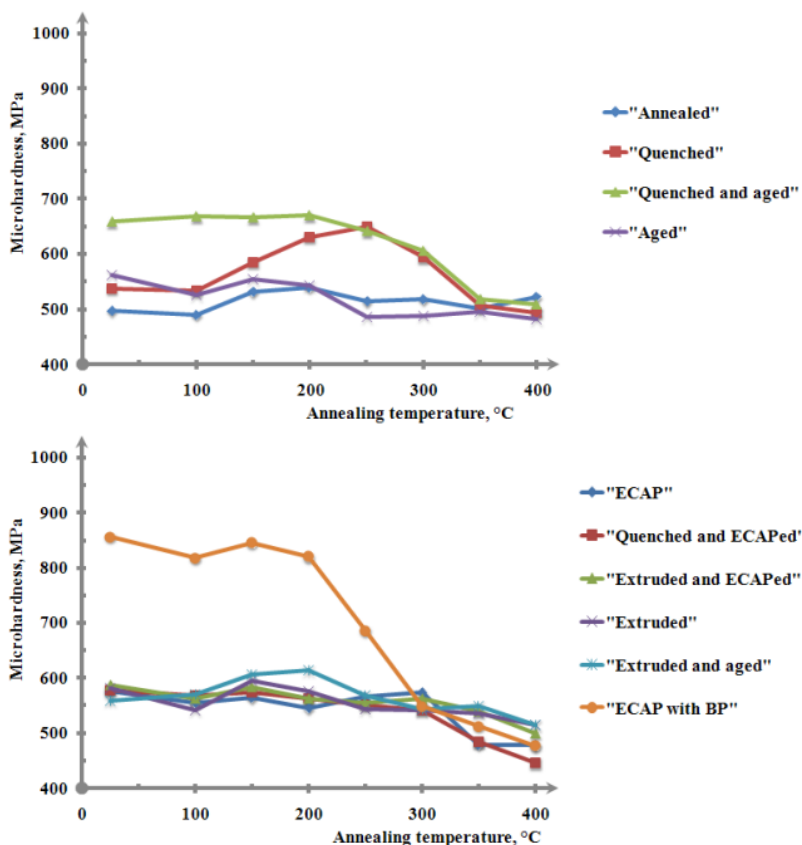
Fig. III.11 Microhardness and thermal stability of the different cast (top) and deformed via extrusion and ECAP (bottom) conditions

Then the specimens were held for one hour at each temperature and the microhardness measurements were performed after every annealing step. Generally it can be mentioned that the high values of microhardness are stable up to 200-250 °C, which is true for the "quenched and aged" or "ECAP with BP" samples. The "quenched" sample exhibited strengthening and the peak of microhardness was observed at 250 °C. At this temperature the value of microhardness was equal to the value of the "quenched and aged" sample. The rest of the samples showed a gradual decrease of microhardness with increasing temperature after 300-350 °C.

<u>Mg-Sm</u>

HPT

Results of the specific electrical resistance and microhardness measurements of the Mg-4.5wt%Sm after various treatments are given in Tab. III.1.

The aging at 300 °C and at 200 °C of the quenched alloy decreased the electrical resistivity due to the decomposition of the supersaturated solid solution. Whereas after aging at 300 °C the drop in the electrical resistance is the highest, due to the full solid solution decomposition [Tab. III.1].

Initial heat treatment	ρ, µOhm·cm / Hv, kg/mm^2		
	Without SPD	SPD at	
		20 °C	200 °C
Quenched	16.2 / 78.4	15.6 / 100.6	14.8 / 104.3
Quenched + aged at 300 °C	11.3 / 81.5	12.1 / 99.6	-
Quenched + aged at 200 °C	12 / 98.5	13.3 / 107.7	-

Table III.1 Specific electrical resistance and microhardness of the Mg-4.5wt%Sm after various treatments

Microhardness measurements showed that compared with aging at 300 °C at 200 °C causes a higher hardening of the alloy as a result of finer Sm-rich precipitates segregated from the Mg solid solution. After aging at 300 °C the microhardness is about the same that as in the as-quenched condition. SPD at both temperatures resulted in significant strengthening of the alloys. The microhardness after SPD at 200 °C is higher and the specific electrical resistance is lower than those after SPD at room temperature, Tab. III.1. It may be ascribed by the partial decomposition of Mg solid solution during deformation at 200 °C, i.e. strain aging [III.2].
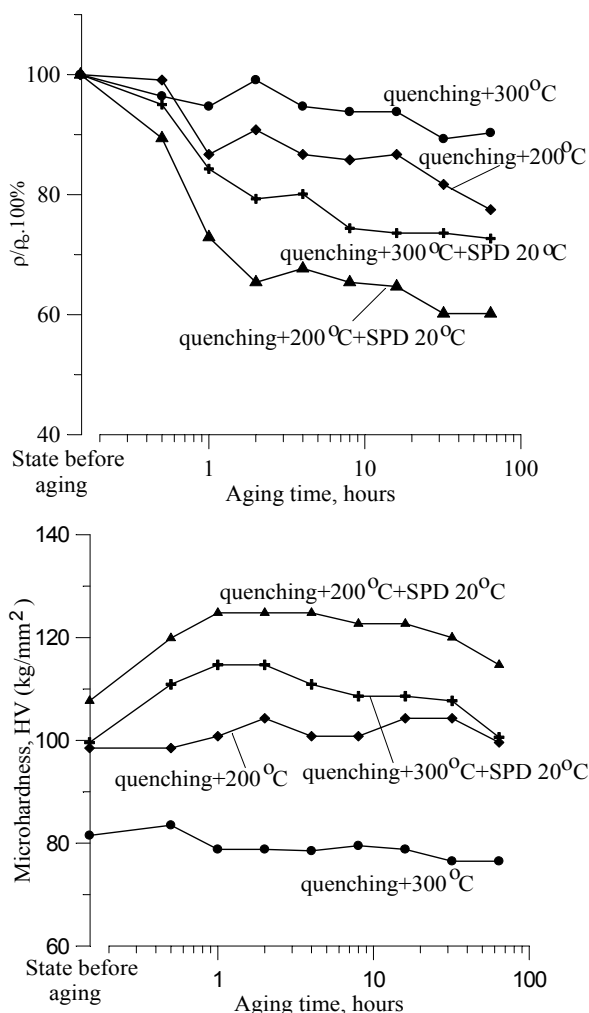
Fig. III.12 Specific electrical resistance (top) and microhardness (bottom) of the Mg-4.5wt%Sm alloy vs. aging time at 200 °C. ρ_0 – is a specific electrical resistance before aging

Four specimens, highlighted with the other color in Tab. III.1, were chosen for the isothermal aging at 200 °C for up to 64 hours, which is shown in Fig. III.12. At this aging temperature, the decomposition of the Mg supersaturated solid solution caused strengthening in the beginning stage and then softening. The specimen quenched and aged at 300 °C performed a little change in the specific electrical resistance and as a result no change in microhardness over the whole

period of subsequent aging at 200 °C. The same alloy processed by HPT exhibited a certain decrease in the specific electrical resistance and some increase in microhardness. The specimen quenched and aged at 200 °C showed a decrease in the specific electrical resistance and increase in the microhardness, but the effect was much higher after SPD was carried out on this sample. The highest strengthening was reached after aging at 200 °C when SPD was applied on the samples pre-aged at 200 °C.

ECAP

Since it was impossible to prepare any tensile test specimens from the ECAPed material, the tensile tests were performed using only the specimens after extrusion and extrusion with subsequent aging. There is no pronounced effect of the aging on the mechanical properties of this alloy. At the room temperature the yield stress is 145 MPa, tensile strength 220 MPa and the elongation to failure of 19% were obtained for the "extruded and aged" condition. At the elevated temperature the yield stress, tensile strength and elongation to failure in the "extruded" condition were measured to be 130 MPa, 180 MPa and 30%, respectively. In Fig. III.13 typical stress-strain curves for the alloy are shown at the initial strain rate 1×10^{-3} s^{-1} on the samples with gauge length 17 mm.
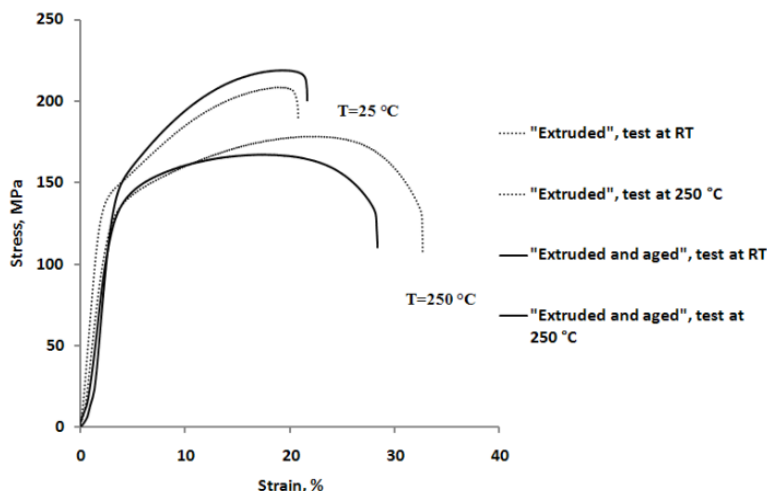

Fig. III.13 Stress-strain curves of the Mg-3.8wt%Sm alloy in extruded condition at room temperature and 250 °C with and without additional aging at 200 °C.

The microhardness measurements were performed on extruded and ECAPed samples, Fig. III.14. The highest value of microhardness is observed for the "ECAP with BP" specimen. It remains relatively stable up to 200 °C and then the rapid softening occurs. The sample in "extruded and ECAPed" condition exhibited a higher microhardness at room temperature, but due to the strengthening effect at 200 °C the "extruded and aged" specimen demonstrates a peak of the microhardness value, which is higher than those of "extruded" or "extruded and ECAPed" conditions.
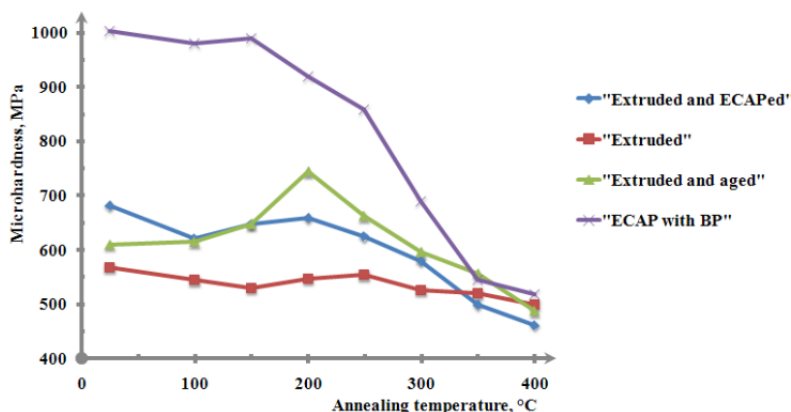
Fig. III.14 Microhardness and thermal stability of the Mg-3.8wt%Sm alloy in various extruded and ECAPed conditions

III.6.   Discussion of the obtained results

The HPT of both Mg-Sm and Mg-Al-Ca alloys led the decrease in the specific electrical resistance and increase in microhardness independent of the preliminary heat treatment. During the following additional aging at elevated temperatures the further increase in microhardness was observed due to the precipitation hardening of the samples after SPD and samples in quenched condition.

Samples of Mg-Al-Ca in the quenched cast condition performed gradual increase in the microhardness, with the maximum reached after 10-20 hours, which indicates on the slow kinetics of the solid solution decomposition, Fig. III.7. However, after the supplementary SPD via HPT the rate and the level of the solid solution decomposition was drastically increased resulting in a sharp drop of the specific

electrical resistance only within an hour. Thus resulting in extra strengthening achieved also in an hour.

The similar behavior of Mg-4.5wt%Sm before and after SPD was obtained. Moreover, the quenched cast condition was already pre-aged at 200 °C, thus showing fewer changes in the specific electrical resistance and microhardness during the following aging at 200 °C, Fig. III.12. But after the supplementary SPD the additional solid solution decomposition was detected during the following aging. Furthermore, the quenched cast condition was pre-aged at even higher temperature of 300 °C, which corresponds to the full decomposition of the supersaturated solid solution. And it was truly reflected in the insignificant changes of specific electrical resistance and microhardness during additional aging at 200 °C. But the supplementary SPD of this state led to the certain decrease in specific electrical resistance showing an additional depletion of Mg solid solution and some increase in microhardness which confirms an additional Mg solid solution decomposition. Thus, the SPD processing via HPT intensifies the decomposition of the supersaturated Mg solid solution and increases its strengthening effect

After the HPT of the Mg alloys the potential of the age-hardening before and after SPD processing was shown. Due to experimental results obtained in the microhardness measurements the corresponding treatments were chosen for the SPD processing via ECAP.

The tensile properties of the Mg-Al-Ca alloy were basically increased. The positive influence of the additional age-hardening on the yield stress and tensile strength can be observed in all conditions, including cast, extruded and ECAPed states, Fig. III.8-9. However, at elevated temperatures it was less pronounced and sometimes performed even some negative changes. Equally negative was the effect of the additional aging on the "quenched and ECAPed" sample, whereas both for the yield and ultimate tensile stresses, which was strange considering the positive background of the increased properties for other samples. It can be ascribed by the relatively high ECAP temperature of 300 °C and long times specimen spent at this temperature, so the full solid solution decomposition did already occur and the softening due to recovery processes happened during additional aging.

The other interesting fact that should be mentioned is the lower strength characteristics of the Mg-Al-Ca alloy after ECAP than after extrusion, though the grain size due to ECAP was measured to be finer. And this tendency was detected for both yield and ultimate

tensile stresses at ambient and elevated temperatures. This phenomenon of texture softening was thoroughly discussed in the last part of the literature review (see Ch. I). During the ECAP processing at the temperatures 250-300 °C, depending on the composition of the alloy the shear texture is evolved. The basal planes are inclined at 45° to the extrusion or longitudinal direction, thus making the shear easier to proceed during the tensile test due to the favorable position of the easy-to-slip basal planes. Hence, lower yield and tensile strengths and higher ductility are usually observed. So, the effect of texture softening overwhelms the strengthening effect due to the grain refinement after ECAP processing.

For the microhardness measurements the texture softening effect does not play such a crucial role, since the deformation is very local and accumulated in a very small volume. Here the values of microhardness observed for ECAPed and extruded conditions are very close, due to the grain size of the same order and similar precipitation level, ~3 μm after ECAP vs. ~9 μm after extrusion, Fig. III.2-3 and 11. But the ECAP processing performed at lower temperature of 220 °C with back pressure resulted in significant improvement of the microhardness, due to the submicron grain size of 500 nm.

The tensile properties of the Mg-3.8wt%Sm were studied only after extrusion with and without additional aging, due to the bad deformability of the alloy via ECAP, Fig. III.13. Strictly speaking, the extrusion was carried out at a very high temperature of 400 °C. The extruded rod performed a rough surface and a bent form, indicating on the incorrect extrusion parameters and the state of the initial material. May be because of the high extrusion temperature the age-hardening effect was not detected on the extruded samples during the tensile tests.

However, the additional aging resulted in higher microhardness of the "extruded and aged" material and further increase of the microhardness due to the additional annealing which led to the peak at 200 °C, Fig. III.14. The same situation with the significant improvement of the microhardness due to the grain refinement down to 300 nm is observed for the sample after ECAP with back pressure at 220 °C. Thus indicating the big difference between the properties obtained after ECAP processing at high and low temperatures.

III.7.   Summary

HPT and ECAP were successfully performed on the Mg-Sm and Mg-Al-Ca alloys in various conditions. The HPT of the both alloy results in the improvement of the microhardness. Additional aging revealed further increase of the microhardness for both alloying systems. The highest value of the microhardness for the Mg-Al-Ca alloy was achieved due to SPD via HPT and additional aging at 175 °C for several hours. The highest strengthening effect for the Mg-Sm alloy can be reached utilizing the HPT at room temperature over the already pre-aged sample at 200 °C for 8 hours with final aging at 200 °C for several hours. It was also shown, that the SPD via HPT intensifies the decomposition of Mg supersaturated solid solution upon aging.

The effect of the aging resulting in enhancement of the mechanical properties was shown for the Mg-Al-Ca alloys. However, due to the texture softening the maximum yield stress of 223 MPa and tensile strength of 256 MPa were obtained at room temperature by the extruded sample after subsequent aging. These values were reduced down to 120 MPa and 155 MPa at the testing temperature of 160 °C, respectively. The elongation to failure was maximal after the ECAP processing both at room and elevated temperatures – 11% and 25%, respectively.

The tensile properties of Mg-Sm alloy after extrusion with and without aging were obtained. No significant influence of the aging was detected on the extruded material.

The microhardness measurements of the Mg-Sm and Mg-Al-Ca alloys revealed the great importance of the ECAP temperature on the quality of the obtained properties. The highest values in both cases were observed by the samples processed at lower ECAP temperature, which was possible due to the applying of the back pressure. The enhanced properties of both alloys were stable up to 200 °C and in some cases they were still retained at 300-350 °C temperatures.

The grain size was reduced after ECAP processing at 300 °C down to 1-3 µm for Mg-Al-Ca and down to 2-5 µm for Mg-Sm alloy. Using the ECAP processing at 220 °C with back pressure provided further grain refinement with the grain size of 200-600 nm for Mg-Sm and 300-800 nm for Mg-Al-Ca alloy.

The HPT and aging showed the great potential on the improvement of the mechanical properties of Mg-Sm and Mg-Al-Ca alloys. In this work the attempt was made to present a transition of the properties attained

for the small samples due to HPT over to the bulk materials obtained after ECAP processing. The possibility of the achieving enhanced properties due to ECAP was shown, though the further work is needed to optimize the existent ECAP facilities in order to lower the ECAP temperature, thus reducing the grain size down to submicron level.

Literature:

[III.1] L.L. Rochlin, "Magnesium alloys containing rare earth metals", Taylor and Francis, London-New York (2003)

[III.2] L.L. Rokhlin, S.V. Dobatkin, T.V. Dobatkina, N.I. Nikitina, M.V. Popov, Mater. Sci. Forum, 503-504 (2006) p. 961

[III.3] S.V. Dobatkin, V.V. Zakharov, L.L. Rokhlin, Mater. Sci. Forum, 503-504 (2006) p. 399

[III.4] L.L. Rochlin, Metally, 2 (2006) p. 104 (in russian)

[III.5] L.L. Rochlin, "Magnievye splavy soderjashie rekozemel'nye metally", M.: Nauka (1980) (in russian)

IV. Enhanced superplasticity of AZ31

IV.1. Introduction

Magnesium alloys have a great potential as structural materials for aerospace, automotive and electronic applications owing to their low density and high strength-to-weight ratio. Furthermore, Mg resources are abundant and Mg products can be recycled more easily compared to polymers. However, the fabrication of magnesium parts using forging, rolling and extrusion is limited due to the relatively low ductility of magnesium alloys. The poor workability of magnesium alloys is explained by their hcp crystal structure. In practice, the development of thermo-mechanical processing leading to significantly enhanced superplastic behavior in magnesium alloys will open up new avenues for industrial applications of plastically-formed magnesium parts.

Of the various commercial Mg alloys, those developed from the Al-Zn ternary system have found the largest number of industrial applications. Among few AZ commercial alloys, the AZ31 alloy represents a good compromise between strength, ductility and cost and is, thus, also one of the most studied alloy of the group. However, even for such widely investigated magnesium alloy there is no consensus concerning the optimum thermo-mechanical processing route leading to enhanced ductility. Generally hot-rolling and extrusion are used [IV.1-6]. Though, in the last decade, broad attention has been given to the use of severe plastic deformation methods (SPD) such as equal channel angular pressing (ECAP) to produce materials with extremely small grains [IV.7] or combination of ECAP with conventional forming techniques [IV.9-10]. At the present time there is no agreement on the type of microstructures most favorable for increasing the elongation-to-failure. The summary of the published results for AZ31 up to date is given in Table IV.1.

Analyzing published results it seems that the severe hot extrusion or hot extrusion followed by the ECAP lead to extensive grain refinement and significantly enhanced superplastic properties with maximum strain of 900% obtained at 300 ºC, [IV.4] and maximum strain of 460% obtained at 150 ºC, [IV.9]. The microstructure of the samples in the almost all published results consists of uniform grains varying in sizes from 0.7 µm to 250 µm.

In this work only ECAP was used for grain refinement of AZ31 magnesium alloy produced by different histories. The parameters of ECAP such as temperature and back pressure (BP) have been

investigated in respect of possible bi-modal structure and enhanced superplastic properties of this alloy.

Ref.	Processing history	Temperature of tensile test, ºC	Strain rate in tensile test, s^{-1}	Eng. strain at fracture, %	Grain size, μm
[IV.1]	Hot-rolling	375	6×10^{-5}	200	-
[IV.2]	Hot-rolling	500	1×10^{-2}	170	250
[IV.3]	Hot-rolling	375	3×10^{-5}	196	130
[IV.4]	Hot-extrusion	200 300	1×10^{-4} 1×10^{-4}	600 900	1 - 4
[IV.5]	Hot-extrusion	177	1×10^{-5}	120	-
[IV.6]	Hot-extrusion	325	1×10^{-4}	608	5
[IV.7]	ECAE	250	3×10^{-3}	400	1
[IV.8]	ECAE	RT	1×10^{-3}	45	-
[IV.9]	Extrusion + ECAE	150	1×10^{-4}	460	0.7
[IV.10]	Rolling + ECAE	500	5×10^{-3}	40	20 - 25

Table IV.1. The summary of publication on superplasticity of AZ31

IV.2. Processing of AZ31 by ECAP with and without back pressure

For the investigations two materials were chosen with different initial states. The first one was cast in Germany with following hot rolling and is described below as "hot rolled" or AZ31(G) material in initial state. No other mechanical or heat treatment was made before ECAP.

The ECAP was performed in Germany, in the Institute of Materials Science and Engineering (TU Clausthal). From the as-received hot-rolled material the ECAP samples with dimensions 10x10 mm^2 and 100 mm in length were prepared. The samples were pressed one after each other, as it is described in Chapter II. In this case no external back pressure was possible to apply at the end of the billet. Thus the samples ECAPed in Germany were pressed without back pressure or very small one created by friction. The temperature of 200 °C and the speed of 10-15 mm/min were selected to perform the extrusion. These are the optimum parameters of a given die design and in respect to initial microstructure. They served to minimize the effect of recrystallization during the processing and thus to achieve the smallest possible grain. Each sample spent about 20 min in average at the working temperature. MoS_2 was used as a temperature resistant lubricant to minimize friction between the die and the samples. After each pass the billets were chilled in the air and grinded back to 10x10 mm^2 in cross section due to elastic springback effect. The Route B$_C$ with the specimen rotation of 90° around the axis after each pass was applied. The billets were pressed for 4, 5 and 6 passes.

The second material was in form of a continuously cast billet produced in Australia and used for ECAP without any additional mechanical treatment. This material is described below as a "cast" or AZ31(A). However, to achieve the most homogeneous microstructure before ECAP processing the specimens have undergone different heat treatments. The samples were held at the temperatures from 350 °C up to 490 °C for different periods of time followed by quenching. The heat treatment was conducted in a furnace in alumina oxide powder to avoid any oxidization.

The ECAP was carried out in Australia, at Monash University in the Department of Materials Engineering. The as-received cast material was cut into cylindrical ECAP specimens with 10 mm in diameter and 35 mm in length. The ram velocity was about 10-20 mm/sec. The specimens were sprayed with a thin graphite layer for better

lubrication before each pass. Prior to extrusion the channel surface in the die was sprayed with the graphite as well and then the whole equipment was heated up to a working temperature for every ECAP pass.

The back pressure (BP) was provided through an additional hydraulic cylinder and applied on the end of the billet in the exit channel during pressing. With the different BP values during ECAP it was possible to extrude the magnesium specimens at different temperatures to find the optimum in respect to processing routes of ECAP. The temperature was varied in the range of 150-250 °C. Generally, the increasing of BP enabled to reduce the processing temperature without any cracking of the material during ECAP for many passes. Since the temperature influence on the microstructure evolution of magnesium during ECAP can not be overestimated, it was very beneficial to decrease temperature during extrusion.

All specimens independent of their heat treatment and deformation history were pressed according route B_C with 90° rotation between each pass for 6 passes totally.

IV.3. Evolution of microstructure during ECAP with and without back pressure

The aimed adjustment and change of the microstructure from the initial state through the certain thermo-mechanical treatment to the end microstructure resulting in enhanced superplastic properties was conducted in two steps, whereas each of them was crucial and peculiar to obtain the best possible elongation to failure. The first step was to achieve the most suitable microstructure prior to ECAP due to homogenization of the cast AZ31(A) alloy. The second step was the ECAP processing under optimum parameters.

The AZ31 is one of the several magnesium alloys that are amenable to age hardening [IV.11]. Thus, several microstructures can be generated via heat treatment. It seems to be, that the other working groups did not study at all or just have not mentioned the heat treatment prior to ECAP regarding the investigations of superplasticity, Tab. IV.1. But in the literature concerning other research topics the adjustment of the microstructure via heat treatment can be found. For instance, in [IV.12] three different microstructures were obtained for AZ31 alloy in hot rolled initial state: single phase with fine equiaxed grains, single phase with coarse grains and twins and fine, equiaxed grains decorated with $Mg_{17}(Al,Zn)_{12}$ grain-boundary precipitates. The

single phase state was achieved after a solution heat treatment at 450 °C for only 1 minute. And the precipitation process in the third microstructure was initiated during a low-temperature aging at 160 °C for three days.

For our investigations, it was substantial to get two initial microstructures with and without precipitates in the cast AZ31(A) alloy. In Fig. IV.1 the metallography of the unetched AZ31(A) after annealing at different temperatures for different periods of time is shown. On the images the particle clusters can be observed even after heat treatment at very high temperatures. The temperature of 300 °C should be already above the solidus temperature known from the literature [IV.13], whereas the eutectic temperatures in the Mg-Al and Mg-Zn binary systems are 436 °C and 340 °C respectively.
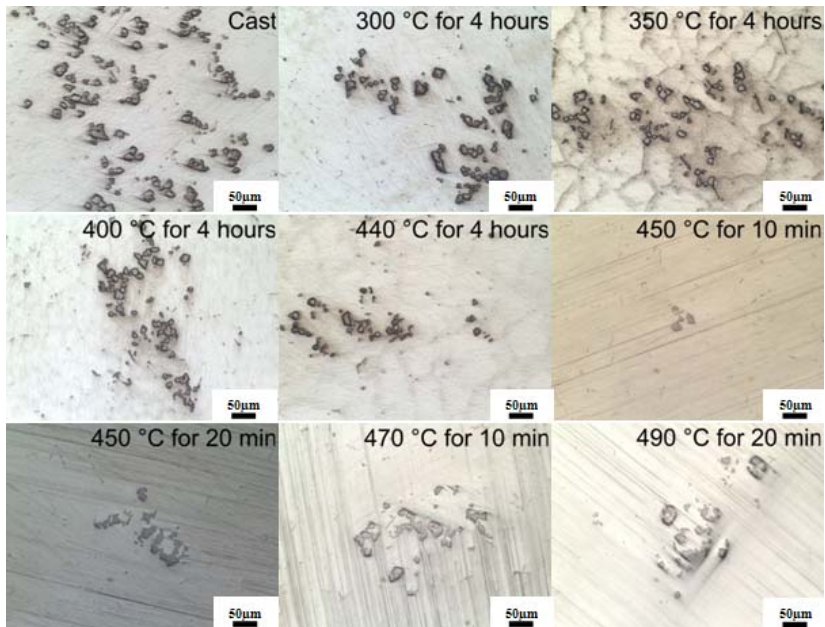

Fig. IV.1. AZ31(A) in as cast state with $Mg_{17}(Al,Zn)_{12}$ particle clusters after different heat treatments

In [IV.11] is written, that the precipitation processes in Mg alloys are frequently complex and are not completely understood. Generally the equilibrium $Mg_{17}Al_{12}$ precipitates segregate from the supersaturated solid solution and are nucleated on (0001)Mg. They are incoherent and their shape is various. It can be needles, plates, globes, angular

shapes or just any irregular forms in chains or clusters. Their size differs as well – the smallest ones can be just dozens of nanometers.

The distribution of the precipitates in the cast material is homogeneous for small and average particles and highly inhomogeneous for the huge particle clusters. Depending on the cut there can be found from one up to several of such clusters, which were formed during crystallization in the regions with increased Al and Zn concentrations. These clusters can reach in size up to several millimeters and can be seen with the naked eye on the cut surface.
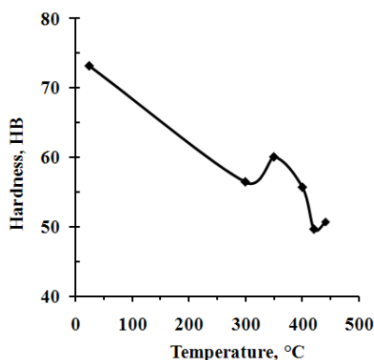

Fig. IV.2. Change of the hardness of AZ31(A) cast after annealing at different temperatures

Since it was impossible to dissolve the precipitations the standard homogenization temperature of 420 °C [IV.13] for cast AZ31(A) was selected. The additionally performed hardness measurements of variously annealed cast approved this temperature, Fig. IV.2. The sample of the AZ31(A) was held one hour at each temperature. The hardness was high at the initial cast state, due to the internal stresses occurred during casting. With the increase of the temperature the stresses were resolved and the hardness became stable after 420 °C.

In Fig. IV.3 the initial microstructures of the AZ31(A) and (G) prior to ECAP are shown. The images were taken also in an unetched condition, to analyse the geometry and distribution of the precipitates.

The difference between the two initial microstructures of AZ31(A) and (G) from the Fig. IV.3 lays in the particles size and their distribution as well as in the grain size. The annealed cast microstructure of AZ31(A) is characterized by huge particle clusters, various shapes of the particles and big grains, with average grain size of about 700 µm. Due to hot rolling the particles in AZ31(G) are distributed more

71

homogenously and the clusters were destroyed. The biggest precipitates are approximately of the same size as in AZ31(A) – up to 25 μm, but their quantity is much lower. They have angular or global shape, while the smaller ones are in form of plates or squares. The average grain size is about 25 μm and there are a lot of zones with twinned grains.
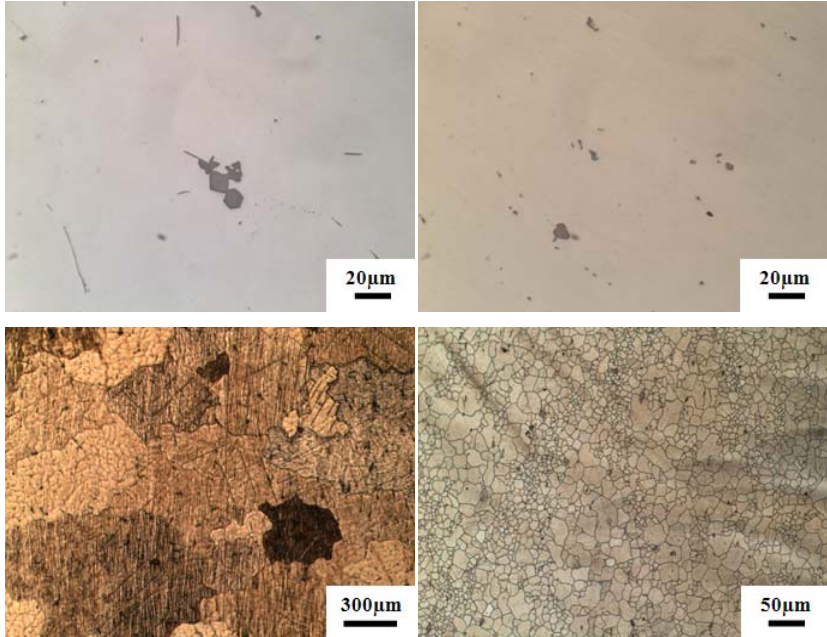

Fig. IV.3. AZ31(A) cast (left) and AZ31(G) hot rolled (right) in unetched (top) and etched (bottom) conditions

Thus, the formability of these two different states is also different, what is crucial for ECAP processing. The material in cast condition possesses much lower ductility than its hot rolled analogue. Moreover, the particle clusters or big particles connected in chains can be the weak link during ECAP, due to their brittleness. The ECAP of such unfavorably formable material was only possible with the help of back pressure (BP). The lowest temperature achieved during SPD was 150 °C with the BP of 218 MPa. The microstructure of the relevant thermo-mechanical treatments were analyzed with the help of optical microscopy (OM) and transmission electron microscopy (TEM). It was the specimens after ECAP with 218 MPa BP at 150, 200 °C and a double step ECAP with 2 first passes at 150 °C and 4 following passes at 180 °C. The latter was chosen as a possible route to obtain

a bi-modal microstructure which is characterized by coexistence of two populations of grains with distinctly different average size and morphology [IV.14]. In the same Ref. is shown, that this type of microstructure can be the reason of extraordinary superplastic ductility.
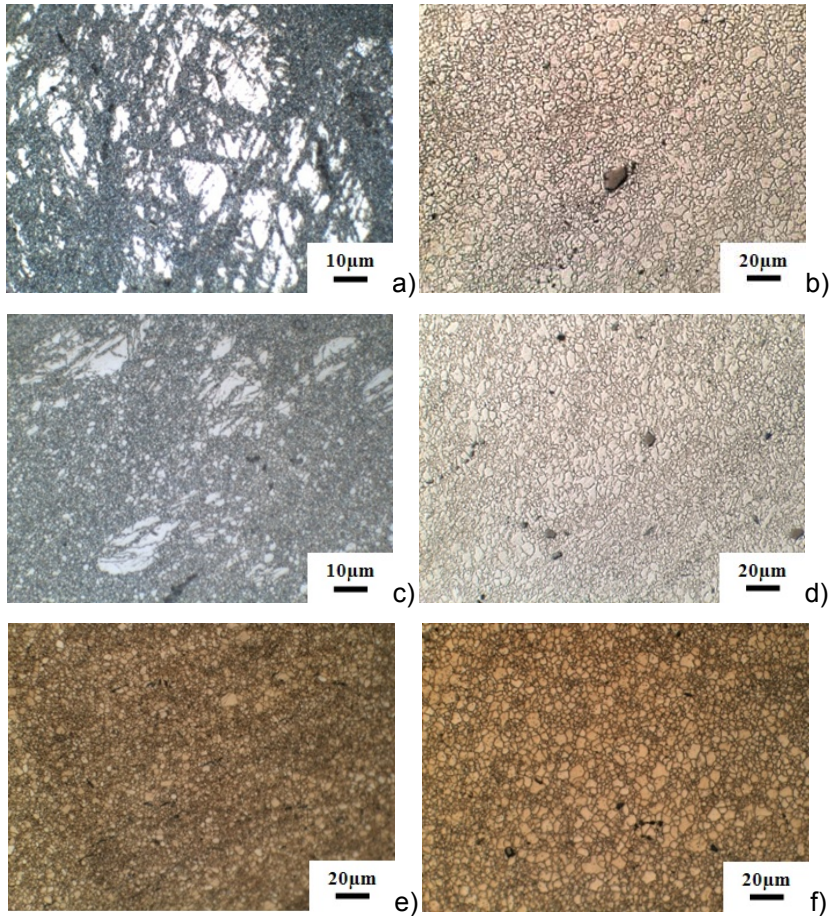

Fig. IV.4. AZ31(A) after different ECAP conditions with 218 MPa BP (left) and AZ31(G) after 4, 5 and 6 ECAP passes without BP (right)

In Fig. IV.4 the typical microstructures in etched condition of AZ31(A) on the left side after different ECAP with BP and of AZ31(G) on the right side ECAPed for 4, 5 and 6 passes at 200 °C without BP are shown. The microstructures after ECAP at 200 °C without BP exhibit the grain size in the same range from 0.5 to 10 μm, with the average

grain size of 1.9 μm, irrespective of the number of passes. The very similar microstructure in respect to the grain size is observed after ECAP at 200 °C with BP, where the average grain size was reduced to 1 μm. The smaller grain size can be explained by the time the specimen spent in the rig at the working temperature after ECAP processing. The ECAP die at Monash University was starting to cool down directly after the pressing and the specimen was removed from the die in couple minutes with consequent quenching, thus the grain growth was inhibited which lead to the smaller grain size in comparison with German specimens.

For these four microstructures the temperature of 200 °C is responsible for the dynamic recrystallization and grain growth during ECAP and it was the determining factor over the grain size parameter independent of BP, number of ECAP passes, ECAP die geometry or initial state of material.

The decrease of the ECAP temperature to 150 °C which was possible due to BP resulted in the bi-modal microstructure (Fig. IV.4.a) and c)), that was very beneficial for the superplasticity. This type of microstructure consists of many zones, where large fractures of the initial grains up to 20 μm are existent. The background is formed by very fine, almost irresolvable in optical microscopy grains. For the closer look the TEM investigations were carried out on the same six microstructures, Fig. IV.5. Their placement corresponds to the one shown in Fig. IV.4. The images d), e), f) obtained from the AZ31(G) after ECAP at 200 °C without BP and are comparable in respect to the grain size.

All four micrographs (b), d), e), f)) show recrystallized, partially recrystallized and deformed grains obtained due to dynamic recrystallization. The first two micrographs in the Fig. IV.5 a) and c) observed on the AZ31(A) specimens after ECAP at 150 °C (a)) and after double step ECAP at 150 and 180 °C (c)) with BP show smaller than 1 μm grain size, approximately 0.5 and 0.7 μm respectively. Such an outstanding result for AZ31 alloy and for Mg alloys generally was possible due to decreasing temperature during ECAP processing thus suppressing the consequences of dynamical recrystallization. The decreased time the Australian specimen spent in the ECAP rig at working temperature was contributive as well.
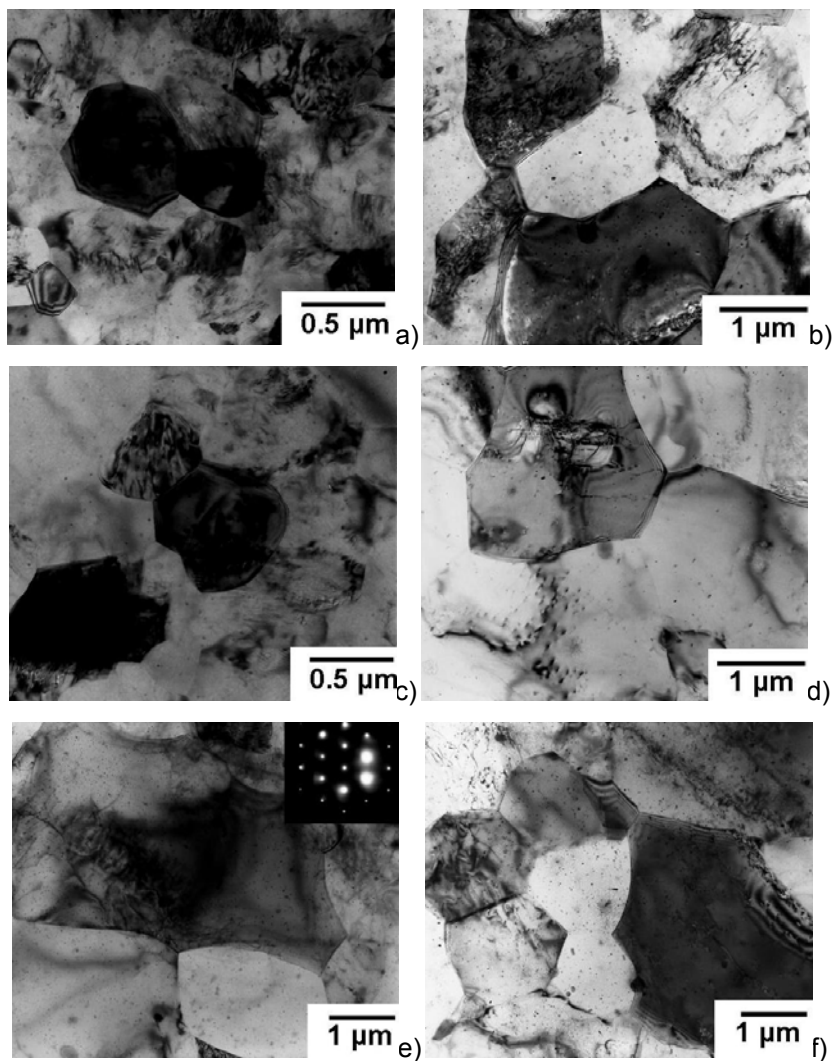
Fig. IV.5 AZ31(A) after different ECAP conditions with 218 MPa BP (left) (a), c), e)) and AZ31(G) after 4, 5 and 6 ECAP passes without BP (right) (b), d), f))

After the successive scale down of the grain size there is still another phase in the AZ31 to investigate, namely precipitates and precipitates clusters. Since the particles in the German AZ31 do not form such clusters as in the Australian one, the latter was chosen to study precipitates evolution from the as cast condition (Fig. IV.1), after

annealing at 420 °C for 4 hours, after ECAP at 150 °C with 218 MPa BP and consequent tensile test, Fig. IV.6. These optical images show the clusters which were formed during melting or casting. They were not dissolved during annealing. Even after severe plastic deformation in form of 6 ECAP passes via route B_C the clusters were not destroyed. On the Fig. IV.6 (right) the working part close to the head of the tensile sample after the optimal thermo-mechanical treatment for superplastic properties is shown. The height of the picture corresponds to the diameter of the tensile specimen near the heads, i.e. if these particle clusters would be found closer to the fracture point they could make the main part of the cross section in the necking point during the test. Thus, in the worst case scenario the clusters can be the reason of the premature failure of the material due to their distribution. In this particular case the sample achieved the biggest elongation to failure of approximately 1200%.
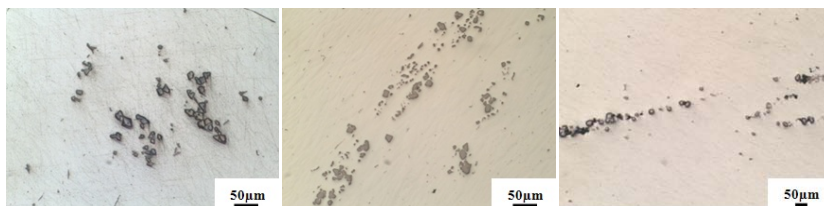

Fig. IV.6. Particle clusters obtained in the same material in as cast state after annealing (left), after ECAP processing (middle) and after tensile test (right)

One tip of this fractured sample was investigated under scanning electron microscopy (SEM) to find out whether any precipitates were on the fracture surface and thus could cause the failure. Fig. IV.7 shows the fracture tip of the sample which was analyzed with the help of Energy Dispersive X-ray Spectroscopy (EDS) but no precipitates of the $Mg_{17}Al_{12}$ phase were found. The fracture occurred without any visible necking, abruptly as a consequence of cavity inter-linkage [IV.15]. The fracture tip exhibits a lot of cavities. Their densities if looking from the side are non-uniform and increase towards the fracture surface. Generally, the samples processed by ECAP appear to contain a higher area fraction of cavities compared to unpressed material.
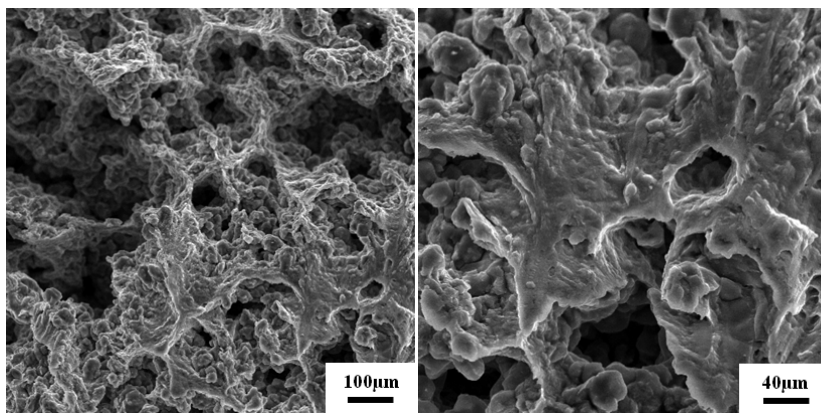
Fig. IV.7. SEM micrographs of the fracture surface of the AZ31(A)
ECAPed at 150 °C with BP after tensile test at 350 °C with 10^{-4} s^{-1}

In the same Ref. [IV.15] one of the basic requirements in order to
achieve superplastic flow in the polycrystalline material is a very small
and stable grain size. The average grain size obtained after analyses
with TEM of the ECAPed material equal to ~0.5 µm is exceptionally
small. To study the grain size stability the optical microscopy of the
specimen after tensile tests were carried out, Fig. IV.8. The material
was taken from the heads of the tensile samples, hence no
deformation did occur during the test. The test temperature was
350 °C, strain rate 10^{-4} s^{-1} and gauge length 8 mm. Since the
elongation to failure of the AZ31(A) specimen was 1200% and of the
AZ31(G) after 6 ECAP passes made up 565% the approximate time
they spent at 350 °C is at least 34 and 15 hours respectively. It is
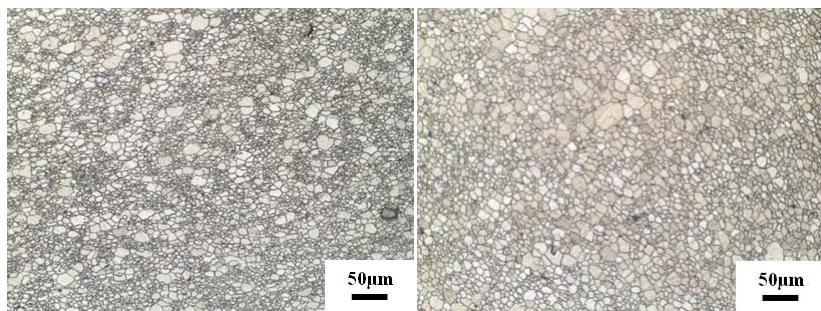apparent that both alloys have stable grain size.

Fig. IV.8. Thermal stability after annealing at 350 °C: AZ31(A)
ECAPed at 150 °C with BP (left) and AZ31(G) ECAPed for 6 passes
at 200 °C without BP (right)

Although there is no precise tensile elongation defining the advent of superplastic flow, it is generally considered that elongations to failure at and above ~500% are indicative of superplastic deformation, as well as the stable grain size [IV.15]. The elongation to failure of both alloys was over 500%, so they both attained superplastic flow. The stable grain size of Australian sample which is with 4.2 µm of factor 3 lower than 12.7 µm of the German one, may be the reason of the higher superplasticity of the Australian sample.

IV.4.   Superplasticity properties of AZ31

After the successful ECAP at various conditions the tensile tests were conducted at different temperatures with different strain rates. The geometry of the tensile test specimens were primarily 8 mm in gauge length and 4 mm in diameter. The only set of German AZ31(G) specimens after 5 ECAP passes and one initial specimen in as-received state from Germany had 10 mm gauge length, but the same diameter of 4 mm. Three diverse strain rates were used: 10^{-2}, 10^{-3} and 10^{-4} s^{-1}.
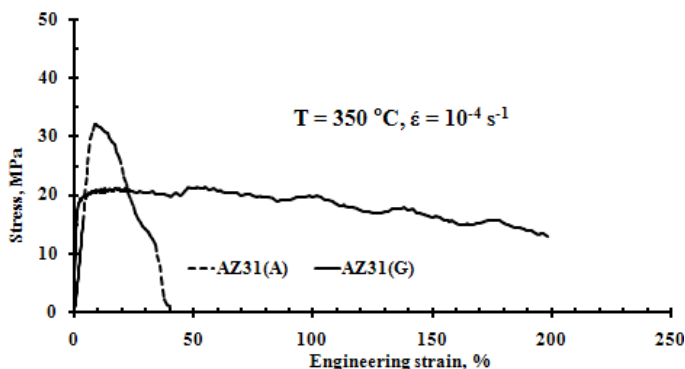

Fig. IV.9. Elongation to failure of as-received unpressed AZ31(A) in cast and AZ31(G) in hot-rolled condition

From the literature it is known, that the magnesium-based alloys exhibit superplastic flow at strain rates which are generally relatively low [Tab. IV.1, Ref. IV.15]. After several tests it was apparent to use the slowest strain rate of 10^{-4} s^{-1} regarding the maximum elongation to failure, Fig. IV.10. In the same figure the evolution of the superplastic properties with the testing temperature is shown as well. The same tests with changing the test temperature and the strain rate were conducted for AZ31(G) specimens, Fig. IV.11.

Both materials show the same tendencies. The elongation to failure increases with the increase of the testing temperature and decrease of the strain rate. Thus the favorable conditions to achieve superplastic flow in AZ31 are the temperature of 350 °C and the strain rate of 10^{-4} s^{-1}. Using these parameters the tensile test was carried out at initial state of both materials to obtain their mechanical properties, Fig. IV.9.
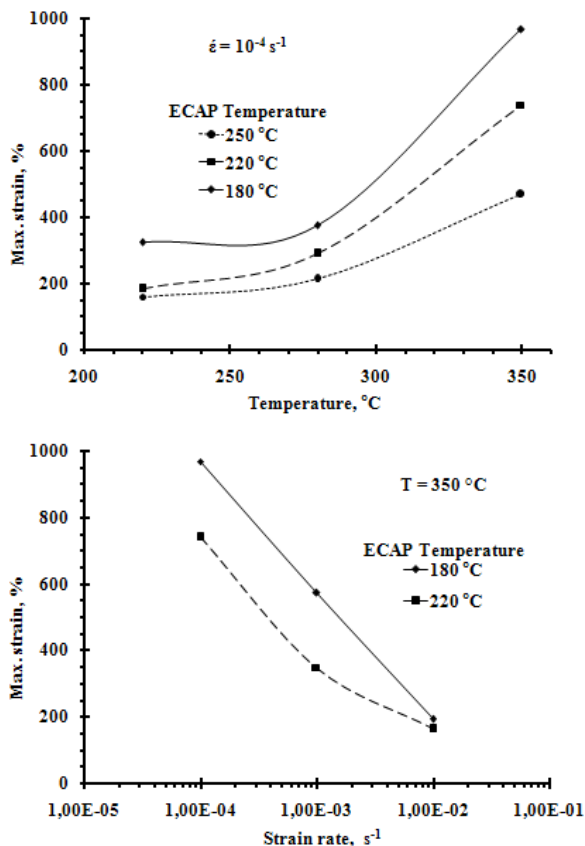

Fig. IV.10. Maximal elongation to failure dependence from the temperature (top) and strain rate (bottom) of the AZ31(A) after different ECAP processing and with various BP

After comparing Fig. IV.9 and 10 it can be shown, that the ECAP does significantly enhance the ability of the material to elongate. The elongation to failure was increased from 40% in initial cast state up to 1000% and more after 6 ECAP passes with BP. The ECAP

temperature itself plays a crucial role in getting the maximum elongation to failure. The latter increases with decreasing of ECAP temperature.
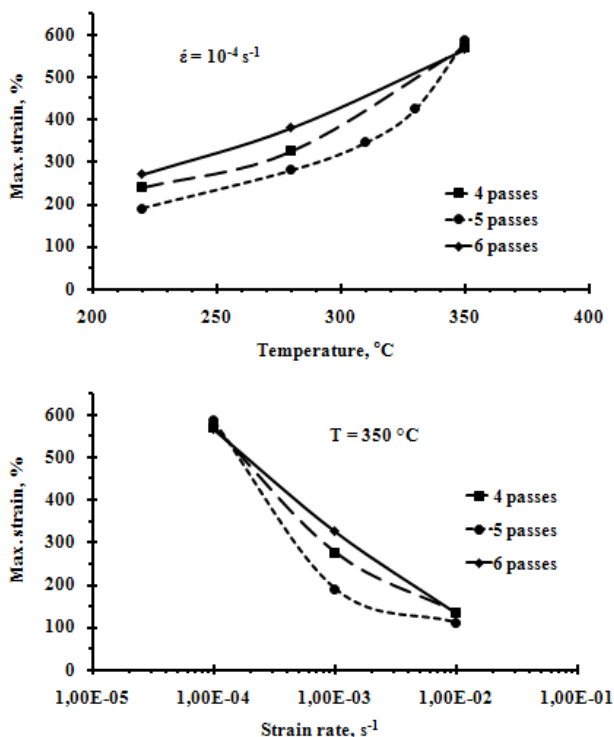

Fig. IV.11. Maximal elongation to failure dependence from the temperature (top) and strain rate (bottom) of the AZ31(G) after 4, 5 and 6 ECAP passes

The ECAP of the hot-rolled material enhanced the superplastic properties and increased the maximum strain from 200% in initial state up to 600% after 6 ECAP passes, Fig. IV.9 and 11. The increase was not as drastic as for the cast material, since the elongation to failure of the hot-rolled material was readily 200%, but it was still raised in 3 times.

The influence of the number of passes on the elongation to failure is not as consistent. As it was discussed earlier, the temperature of 200 °C for ECAP processing plus the long time specimen spent at the working temperature without consequent quenching was the determining factor for the grain size. The tendency of the curves in

80

Fig. IV.11 for the specimens after 4 and 6 ECAP passes is similar. The slightly different values for the specimen after 5 ECAP passes can be explained with the other geometry of the tensile test samples. Generally, the elongations increase with increasing number of passes which corresponds the increase of the fraction of high-angle boundaries [IV.15].

Since the ECAP at 180, 220 and 250 °C for AZ31(A) and at 200 °C for AZ31(G) was made, it became obvious that the presence of back pressure gives not only a better result regarding superplasticity already at higher temperature in comparison to the ECAP without BP but also allows further reduction of ECAP temperature, which leads to a further enhancement in superplastic behavior, Fig. IV.12.
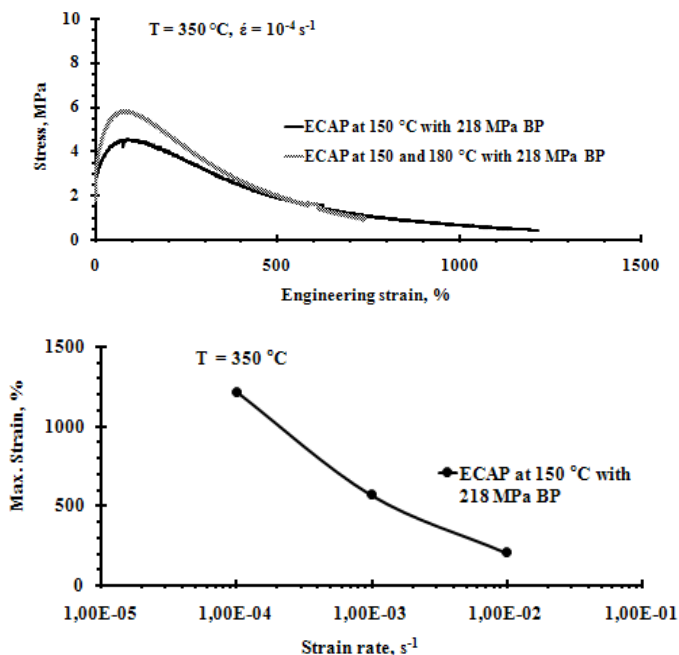

Fig. IV.12. AZ31(A), strain-stress curves (top) and strain rate (bottom) dependence of the maximal elongation to failure at constant temperature of 350 °C

The record superplasticity of 1215% was achieved for AZ31 that was ECAPed at 150 °C for 6 passes with BP after casting. The temperature of ECAP was decreased to 150 °C, due to application of

the higher level of BP, which led to a bi-modal grain structure with big fractures of old grains and very fine new grains appeared as a result of severe plastic deformation, Fig. IV.3.
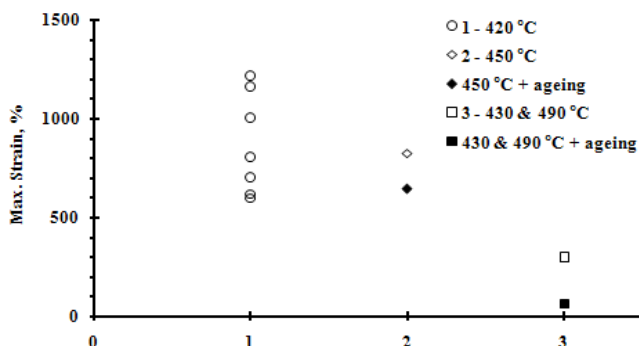

Fig. IV.13. AZ31(A) after ECAP at 150 °C with 218-262 MPa BP after different heat treatments. Increase in the number of heat treatment corresponds the increase in the annealing temperature. The solid points are for the heat treatment with consequent aging at 160 °C for approximately 1 day

The Fig. IV.13 shows the maximal elongations after different heat treatments. The first one is the heat treatment that was used for the major part of the specimens. It is annealing at 420 °C. The second and third ones were the attempts to dissolve precipitates in the Mg solid solution, Fig. IV.1. The second heat treatment was made at 450 °C for a short time, at the temperature that is slightly higher than eutectic temperatures in the Mg-Al, Mg-Zn binary systems. The third heat treatment was a double step annealing with the first temperature of 430 °C that is below the respective eutectic temperatures. This step should have dissolved the precipitates and their clusters at the Mg solid solution. And during the next step at 490 °C the diffusion should have equaled the higher concentrations of alloying elements around particle clusters over the whole specimen volume. All heat treatments were followed by quenching to avoid any precipitation.

According to these results the homogenization temperature of 420 °C was chosen properly. The higher then the temperature and the longer the annealing time was the lower became the elongation to failure. And the additional aging only worsened the result. For the main heat treatment there are many data points plotted on the graph. It is a big scattering, but not so unusual for magnesium alloys [IV.13]. It can be explained in terms of internal failures occurred during casting, which

did not propagate through ECAP processing due to the high hydrostatic pressure (BP) or with the presence of huge particle clusters, that can randomly get into the necking point.

Anyway, after the ECAP processing independent of the initial state in material the superplasticity was achieved for AZ31. It can be concluded that the ECAP temperature under 250 °C gives a favorable microstructure with the grain size small and stable enough to obtain elongations to failure from 500% and higher. The ECAP in a 90° die is possible at temperatures as high as 200 °C. The further reduction of the pressing temperature leads to the cracking of the material. Still using some add-ons like back pressure, another die geometry and keeping the specimen only for a short time of deformation at the working temperature allows to decrease the ECAP temperature down to 150 °C. Such optimization of ECAP refines the microstructure and enhances the superplasticity more than twice, Fig. IV.14.
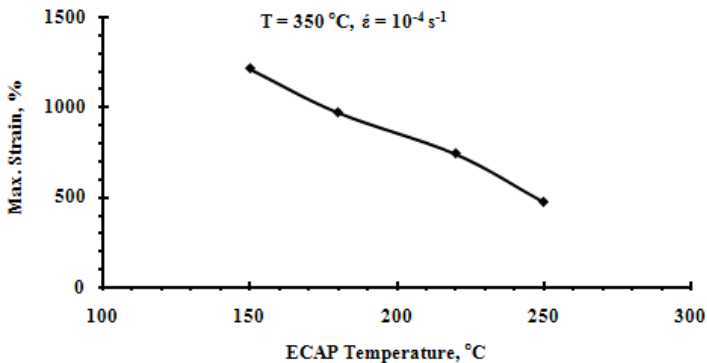

Fig. IV.14. Influence of ECAP temperature on the superplastic properties of AZ31(A)

In the Ref. [IV.16] the Mg-8% Li alloy was pressed for 10 passes without BP using ECAP die with a channel angle of 135°. The pressing was possible at room temperature, due to the bigger angle and thus lower strain imposed in ECAP. Since the grain growth and recrystallization processes were completely hemmed, the microstructure was refined with a very high degree. Therefore an exceptionally high elongation of ~1780% was achieved. Following this trend, there is still a lot of space for further optimization of ECAP processing and its parameters. The increase of the die angle with the opportunity to apply BP for providing more homogeneous shear zone

may result in decreasing of the ECAP temperature, which can expand the borders of today's superplasticity for magnesium alloys.

IV.5. Summary

The ECAP was successfully applied to AZ31 magnesium alloy under various conditions. The AZ31(G) in hot-rolled initial state was possible to press at temperatures as low as 200 °C for 6 ECAP passes via route B_C without getting material cracked. After ECAP the microstructure was refined from 25 µm down to 2 µm. It was shown that the determining factor in microstructure evolution during ECAP processing was temperature, if the latter is equal or higher than 200 °C. The obtained grain structure was stable and exhibited good superplastic behavior. The elongation to failure was enhanced from 200% in hot-rolled condition up to ~560% after pressing.

The influence of the number of ECAP passes on the superplastic properties of the AZ31(G) can be compared between 4 and 6 passes, because the tensile test specimens had the same geometry. For low test temperatures up to 300 °C the elongations to failure of the 6 times ECAPed specimen are slightly higher, however at the test temperatures above 300 °C the difference is negligible.

The AZ31(A) in cast condition was pressed at the range of temperatures from 150 to 250 °C. The ECAP was carried out using route B_C, the material was pressed for 6 times and various BP was applied. The lowering of the ECAP temperature was possible due to the presence of BP. The lower the pressing temperature was the higher should have been the back pressure force to preserve material from cracking. After the successful ECAP at 150 °C the microstructure was refined from ~700 µm in cast down to 0.5 µm in pressed condition. The bi-modal grain structure was obtained. The grain size remained stable even after 1.5 days of staying at working temperature, which was >0.5Tm, namely 350 °C.

It was shown, that with the decrease of the ECAP temperature the elongation to failure was increased from the insignificant 40% in cast up to the record for this alloy 1215% in pressed condition. It has to be mentioned, that ECAP was performed on the cast alloy without any mechanical treatment prior to ECAP.

For both materials, independent of the ECAP conditions and initial state the same tendencies were found. The elongation to failure increases with the increase of the testing temperature and decrease of

the strain rate. The optimum testing parameters regarding superplasticity were found to be T = 350 °C and $\dot{\varepsilon}$ = 10^{-4} s^{-1}.

Literature:

[IV.1]   H. Watanabe, H. Tsutsui, T. Mukai, K. Ishikawa, Y. Okanda, M. Kohzu, K. Higashi, Mater. Sci. For., 350 (2000) p. 171

[IV.2]   X. Wu, Y. Liu, H. Hao, Mater. Sci. For., 357-359 (2001) p. 363

[IV.3]   H. Watanabe, H. Tsutsui, T. Mukai, M. Kohzu, S. Tanabe, K. Higashi, International J. of Plasticity, 17_3 (2001) p. 387

[IV.4]   H.K. Lin, J.C. Huang, Mater. Trans., 43.10 (2002) p. 2424

[IV.5]   A. Bussiba, A.B. Artzy, A. Shtechman, S. Ifergan, M. Kupiec, Mater. Sci. Eng., A302_1 (2001) p. 56

[IV.6]   H. Watanabe, T. Mukai, K. Ishikawa, Y. Okanda, M. Kohzu, K. Higashi, Keikinzoku, J. of Japan Institute of Light Met., 49_8 (1999) p. 401

[IV.7]   V.N. Chuvil'deev, V.I. Kopylov, M.Yu. Gryaznov, A.N. Sysoev, Doklady Akademii Nauk, 391_1 (2003) p. 47

[IV.8]   T. Mukai, M. Yamanoi, H. Watanabe, K. Higashi, Scripta Mater., 45_1 (2001) p. 89

[IV.9]   H.K. Lin, Huang, C, Jacob, T.G. Langdon, Mater. Sci. Eng., A 402.1-2 (2005) p. 250

[IV.10] S.R. Agnew, T.M. Lillo, J. Macheret, G.M. Stoica, L. Chen,Y. Lu, D. Fielden, P.K. Liaw, TMS Annual Meeting (2001) p. 243

[IV.11] I.J. Polmear "Light Alloys" Second Edition, ISDN 0-340-49175-2 (1989) p. 170

[IV.12] M. Marya, L. G. Hector, R. Verma, W. Tong, Mat. Sci. Eng., A418 (2006) p. 341

[IV.13] Magnesium-Taschenbuch, Aluminium-Zentrale Düsseldorf, Aluminium-Verlag, Düsseldorf, First Edition (2000)

[IV.14] R. Lapovok, R. Cottam, P. Thompson and Y. Estrin, J. Mater. Res., 20 (2004) p. 1375

[IV.15] M. Kawasaki, T.G. Langdon, J. Mater. Sci., DOI 10.1007/s10853-006-0954-2

[IV.16] M. Furui, H. Kitamura, H. Anada, T.G. Langdon, Acta Mater., 55 (2007) p. 1083

V. Change in kinetics of hydrogen storage of Mg-Ni alloy due to ECAP

V.1. Introduction

A hydrogen economy is an imaginary close future economy in which energy, for mobile applications, such as vehicles and aircraft, as well as for electrical grid load balancing i.e. daily peak demand reserve, is stored as hydrogen, H_2. It might serve as an environmentally cleaner way to deliver energy without release of pollutants: emission of greenhouse gases and other harmful substances. But to use all of the new energy storage medium benefits a hydrogen storage material or system for mobile applications according to safe and reliable transportation of hydrogen has to be found. There are some competitive solutions in this area, which could be divided into two groups. The first group characterizes hydrogen in a bonded form, such as ammonia storage, metal hydrides, synthesized hydrocarbons and more exotic hydrogen carriers based on nanotechnology - carbon buckyballs and nanotubes or their combination with metal hydrides. And the second one consists of the hydrogen itself in its pure form: high pressure tanks or liquefied hydrogen.

As far as the hydrides are a real and safe alternative to the other hydrogen storage mediums they can be divided into simple hydrides of magnesium or transition metals and complex metal hydrides. The Mg-based hydrides gained a great deal of attention due to their low costs, low density and large abundance in the earth's crust. The ability of pure Mg to reversibly store up to 7.6 wt.% in the form of MgH_2 is a sufficient advantage. However, slow hydrogen absorption and desorption kinetics and high operating temperatures are the disadvantages to overcome before practical use in automobile industry.

Hydrogenation kinetics is related to the dissociation of molecular hydrogen into the metal. Because of the low dissociation ability of Mg for hydrogen molecules and very slow diffusion of the atomic hydrogen in Mg numerous attempts were made to improve hydrogenation and dehydrogenation kinetics by refining the microstructure [V.2-4] or adding catalytic materials [V.1, 2]. Many catalytic additions to pure Mg can be used for enhancing the hydrogenation kinetics – Ni, Ti, Fe, Pd, V, Nb_2O_5 and Mn [V.1-3 and 5]. Additive atoms play the role of a catalyst assisting the dissociation of H_2 molecules on the surface and lowering strength of Mg-H bonds

[V.1]. However, all these attempts led to improvement of hydrogenation kinetics only and failed to change the thermodynamics of Mg-H interaction [V.1-4 and 6].

The Mg-Ni alloy was chosen as a hydrogen storage medium due to his commercial availability. It is based on Mg_2Ni intermetallic compound that desorbs hydrogen at 1 atm at the temperature of 255 °C, which is lower in comparison to pure Mg with 279 °C. But the gravimetric storage capacity of Mg_2Ni is only 3.6 wt.% what is about twice as low as for pure Mg.

The hydrogenation kinetics and thermodynamics are very sensitive to every defects, chemical disorder and internal strain [IV.1]. Such changes could be introduced through severe plastic deformation, SPD. Equal channel angular pressing, ECAP is one of the most successful methods to obtain ultrafine grain structure in bulk materials, i.e. in this case enough material for commercial use.

V.2.   ECAP processing of the eutectic Mg-Ni alloy

An eutectic alloy of the composition $Mg_{89}Ni_{11}$ in cast state was selected to perform the experiments. The ECAP was done in the Institute for Materials Science and Engineering (TU Clausthal). The as-received cast material was cut into ECAP samples with dimensions of 10x10 mm^2 in cross section and 60 mm in length. After each pass the samples were chilled in the air and grinded back to the 10x10 mm^2, because of the elastic springback effect. The route B_C was used, i.e. every sample was rotated for 90° around its axis between the passes. As the specimen was set inside the preheated die several minutes were left to let the specimen achieve the working temperature. After the pressing process was over, another specimen was put into the channel and during the next pressing the first one was pressed out. The average duration of the one pass cycle is about 15 min, i.e. all this time the specimen reside at the working temperature. The pressing speed was 10-15 mm/min.

Different temperatures were tried out to perform the ECAP. Mg belongs to the materials with hexagonal close packed (hcp) structure and at the room temperature there are not enough active slip systems. Moreover, the ductility of the cast materials is very low. Thus the first successful temperature was 300 °C to obtain material without cracking. Through the next several passes the microstructure was refined and the ductility and formability of the material was enhanced. Since that it was possible to reduce temperature, to avoid

unnecessary recrystallization and to keep the structure in ultrafine condition. So, during the ninth and tenth pass the temperature was decreased to 240 and 230 °C respectively. A temperature resistant MoS_2 lubricant was employed to minimize the friction between the billet and the die. After ECAP the material was highly reactive and, in presence of humidity or in contact with water the surface was immediately covered with foam, so special care in sample storage and preparation for microscopy investigations was required.

V.3.   Microstructure changes due to ECAP

The $Mg_{89}Ni_{11}$ alloy consists of two phases. After X-ray analysis Mg and Mg_2Ni phases were found in the initial as cast alloy and the alloys processed by ECAP. However after ECAP the relative intensities of the peaks were changed and some peak broadening occurred [V.7].

In Fig. V.1 the TEM bright field images of typical microstructures of the as cast and ECAPed samples are shown. These micrographs characterize the microstructure evolution from the as received material to the ECAPed one.

In the eutectic lamellar structure the lamellae of brittle Mg_2Ni phase are embedded in more ductile surroundings of Mg-based solid solution. On the TEM image with high magnification it looks like continuous sheets in the longitudinal direction and thin layers in the perpendicular direction. So, the grain size in longitudinal way is up to 10 and more micrometers and less than a micron in thickness. On the TEM images is shown that the microstructure was changed from lamellar in the as-cast state to ultrafine grained one after 10 ECAP passes, due to the breaking of these lamellae structure. After ECAP the Mg_2Ni grains are homogeneously distributed in extruded samples, whereas each phase is surrounded with the other one. The grain size for Mg phase and for Mg_2Ni grains ranges from 0.5 to 1 µm and from 0.5 to 2 µm respectively. Though the TEM studies also show presence of some anomalously large grains of Mg_2Ni with the size of several microns. As a result the obtained microstructure is significantly finer than in as cast samples, which shows the efficiency of ECAP in reducing the grain size to sub-micrometer size. The high dislocation density in Mg phase was observed in ECAPed samples.
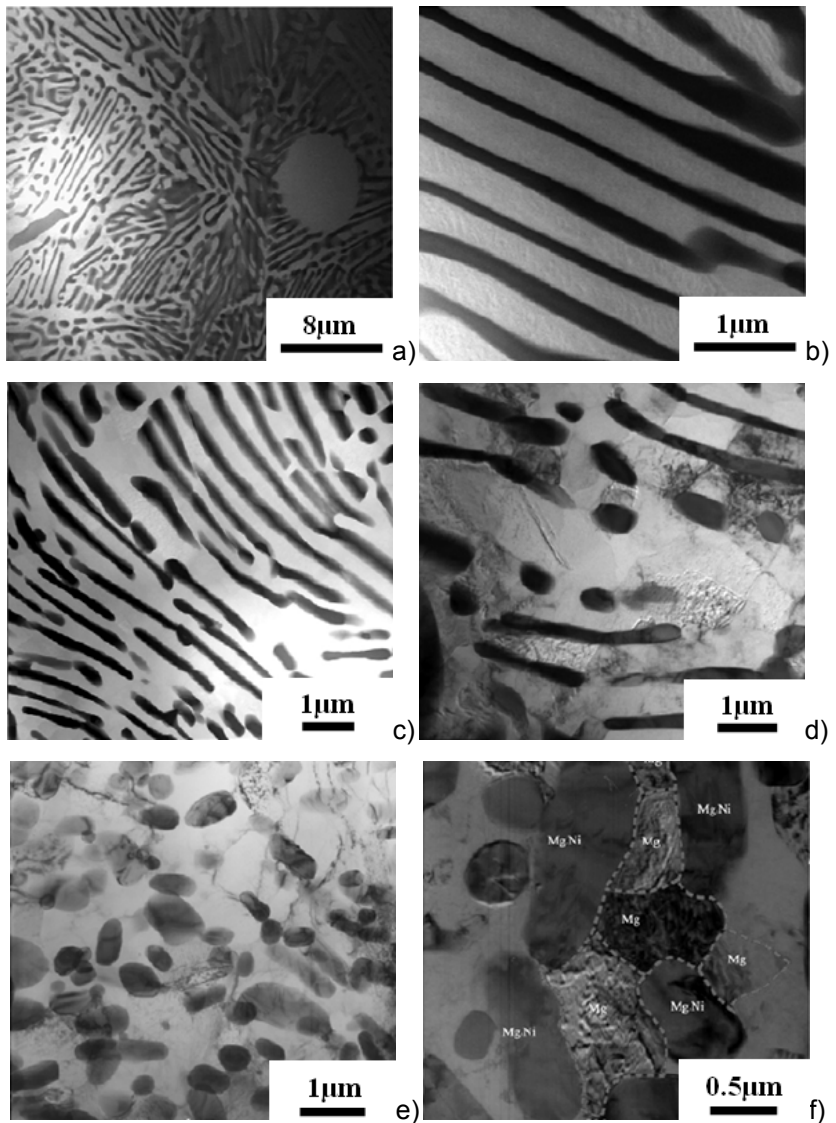
Fig. V.1. Bright field TEM micrographs of the as cast sample (a, b), the sample processed by 1 ECAP pass (c, d) and the sample processed by 10 ECAP passes (e, f). The dashed lines in (f) serve as a help for recognizing the individual Mg grains

To study the composition of the alloy phases and on specified places Energy Dispersive X-ray Spectroscopy (EDS) and Electron Energy

Loss Spectroscopy (EELS) methods were used. The EDS investigations in TEM of the as cast sample showed that the composition of Mg_2Ni lamellae corresponds to the stoichiometric formula, while Mg lamellae exhibited some homogeneously distributed dissolved Ni at the concentration level close to the detection limit of EDS, which is approximately 0.2 at.%. After 10 ECAP passes material exhibits the same stoichiometric constitution for the large Mg_2Ni grains, but some excess of Mg in sub-micrometer particles in comparison to the as cast samples. Regarding Mg grains after ECAP different Ni distributions were observed. In the interior of the grains the Ni concentration was very close to the detection limit of EDS, while in the vicinity of Mg_2Ni grains it was in the range of 0.5-1.0 at.%. Moreover, the Ni concentrations in the Mg grains with high dislocation density were consistently higher than in the grains with lower dislocation density. The presence of Ni in Mg grains was also confirmed by EELS, whereas according to the equilibrium Mg-Ni phase diagram the solubility of Ni in Mg at room temperature is negligibly small [V.8].

In Fig. V.2 the SEM micrographs of the particles of the alloy processed by 10 ECAP passes after repeated hydrogen absorption-desorption cycling are shown. From one side the rasped particles preserved their mechanical integrity and from the other side, the surface of the particles at higher magnification appears rough, porous and fragmented. Cracking and decohesion along Mg-Mg_2Ni interfaces and grain boundaries occurred during hydrogenation. Due to such fragmentation the surface to volume ratio was significantly increased, which should accelerate the hydrogenation kinetics. The average size of these individual fragments is about one micrometer.

From the literature it is known that no grain refinement below 100 µm has been achieved with the ECAP of pure Mg [V.9]. The main reason for this is dynamic recrystallization that occurs during SPD at elevated temperatures, which limits the potential of this processing technique for microstructure refinement, especially for Mg. However, alloying Mg with other elements helps to suppress dynamic recrystallization and reduce the mobility of grain boundaries thus inhibiting grain growth. Sometimes, even the addition of small amount of alloying element could help to decrease ECAP temperature and, consequently, the final grain growth. In [V.9] as a result of adding 0.9% of Al to Mg the grain size after successful ECAP at lower temperature was reduced to 17 µm. Through adding of more alloying elements or by increasing their content in Mg further grain refinement can be achieved. The very low average grain sizes of 0.5 µm [V.10 and 11] and 0.8 µm [V.12] have been reported in the alloys of AZ series, containing Al, Zn and

Mn. Hence, the achieved average grain size of 0.8 µm for Mg-Ni belongs to the lowest reported for ECAPed Mg alloys.
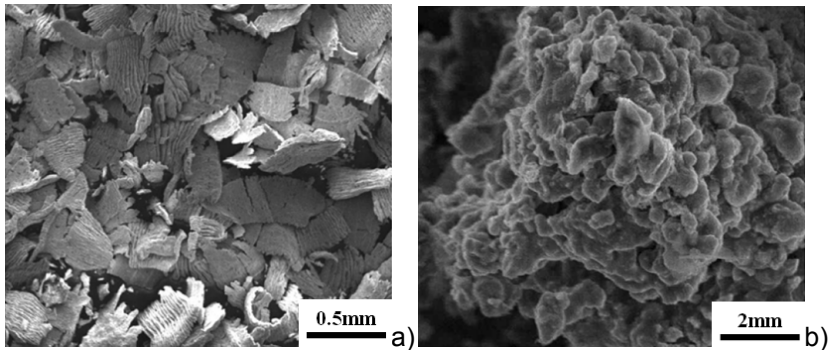

Fig. V.2. SEM micrographs of rasped particles of the sample processed by 10 ECAP passes (a) and after following hydrogenation/ dehydrogenation cycling (b)

This outstanding result in the microstructure refinement was possible through the ECAP parameters optimization as well as by the adding of an alloying element, in this case Ni. Firstly, the initial lamellar structure in as cast alloy with the average distance of about 0.5 µm was broken during ECAP. Since the Mg_2Ni lamellae are harder and possess over the higher thermal stability than Mg ones and the ECAP process introduces a very homogeneous deformation, they were transformed into the consistently distributed particles. They did not experience at all or in a very low degree grain growth and consequently served as the barriers preventing extensive grain growth in Mg phase.

Secondly, due to intensive plastic deformation during ECAP a metastable supersaturated Mg(Ni) solid solution was formed. Such additional Ni atoms in Mg phase interact with the migrating grain boundaries and may impede their motion and suppress the processes of dynamic recrystallization.

The formation of the metastable solid solution during ECAP could be explained in terms of diffusion. According to EDS observations the process of chemical interdiffusion at the Mg/Mg_2Ni was initiated and accelerated by ECAP at elevated temperatures. In the [V.7] some calculations to estimate the characteristic size of the Ni diffusion zone in Mg are given. Regarding the diffusion of Ni in Mg at the temperature of interest, the short circuit diffusion along the dislocation lines and the grain boundaries as well as these both diffusions during the following ECAP passes at lower temperatures a reasonable estimate was made

with a good correlation to the EDS measurements, which indicate an increase Ni concentration in Mg grains at the distances of 100-200 nm from the Mg_2Ni, the Ni source grains.

There can be several reasons for formation of supersaturated solid solution. Thermodynamically, due to the disordered nature of grain boundaries and dislocations cores after ECAP in Mg phase the equilibrium solubility of Ni within them can be much higher than in the bulk. Also the appearance of mobile solute-vacancy pairs consisting from Ni atoms and excess vacancies formed during ECAP can contribute to the non-equilibrium solubility of Ni in Mg phase. From the other side, because of the instantaneous nature of the microstructure formation during ECAP at elevated temperatures some Ni atoms diffusing along gliding dislocations and migrating grain boundaries can be left behind in Mg matrix, thus contributing to the formation of supersaturated solid solution.

A similar non-equilibrium behavior of cementite resulted in complete dissolution of the last one in pearlitic steel during high pressure torsion [V.13]. Generally, the formation of the supersaturated solid solutions during SPD is not uncommon [V.14] but in our case the presence of this fact is crucial for understanding the hydrogenation properties of processed alloys.

V.4.   Improvement of hydrogen storage capabilities of Mg-Ni alloy

For hydrogenation studies the samples were comminuted by filing with a rasp, which resulted in the particle sizes in the range of 0.5-1 millimeter. This procedure itself is additional deformation, so that some modification of microstructure can occur in an as cast sample, while no changes in microstructure of ECAPed samples are expected.

The capacity method (Sievert's method) is used as a method of measuring the hydrogen storage capacity and reaction rate of Mg-Ni alloy. In this method, the hydrogen storage capacity is calculated from the pressure change before and after the equivalence state of two containers of already-known capacity, reservoir and reactor.

After rasping the powder samples of 1±0.15 g weight were placed in a stainless steel reactor with the internal volume 21±1 cm^3. It was heated by external resistance furnace and the temperature was controlled by an embedded chromel-alumel thermocouple with

accuracy of ±0.5 °C. The mass ratio of the sample and the hot reactor was approximately 1:200.

Prior to determine PCT diagrams all samples were hydrogenated with 99.99999 at.% purity hydrogen at 300 °C and hydrogen pressure of 25 atm, and then processed by five desorption-absorption cycles. No thermal activation prior to hydrogenation was needed.

The rate of desorption from the sample fully saturated with hydrogen was measured after determining the PCT diagrams. The sample was hold in initially vacuumed system. After heating the sample up to the temperature of 300 °C, which was the beginning temperature of the desorption process, the initial pressure was measured. At the next step the valve that separates the reactor from the reservoir was opened and the desorption process was initiated. At the end of it the hydrogen pressure was measured and considering the initial pressure the pressure change of the system was calculated.

In Fig. V.3 (top) the PCT isotherms of as cast and ECAPed samples at 300 °C are shown. For better interpretation the diagrams can be divided into two parts, a low-H part and a high-H part. According to the quantity of absorbed hydrogen up to 5 wt.% such pressure plateau parts can be attributed to the Mg grains. In fact these parts have usually negligible hysteresis. While the pressure plateau parts with the hydrogen concentration from 5 wt.% to 6-6.5 wt.% are associated with the absorption of Mg_2Ni phase and they exhibit strong pressure hysteresis.

In the low-H part the alloy processed by 10 ECAP passes presents the highest equilibrium hydrogen desorption pressures in the range of 2-3 atm. PCT diagrams of the samples after ECAP exhibit a tilted plateau and the slope of the plateau increasing with increasing number of ECAP passes. The pressure plateaus are tilted for all temperatures for ECAPed material, which is shown on the pressure-composition (PC) diagrams at different temperatures in Fig. V.3 (bottom). For three highest temperatures 280, 300 and 325 °C the desorption branches of the pressure plateaus do not exhibit any discontinuities or changes of slope at the transition from hydrogenation of Mg to Mg_2Ni phase. For instance such discontinuities were observed in all previous studies of the hydrogenation of Mg-Ni alloys [V.1 and 3]. And even at the highest temperature of 325 °C the tilt in pressure plateau associated with Mg does not disappear.
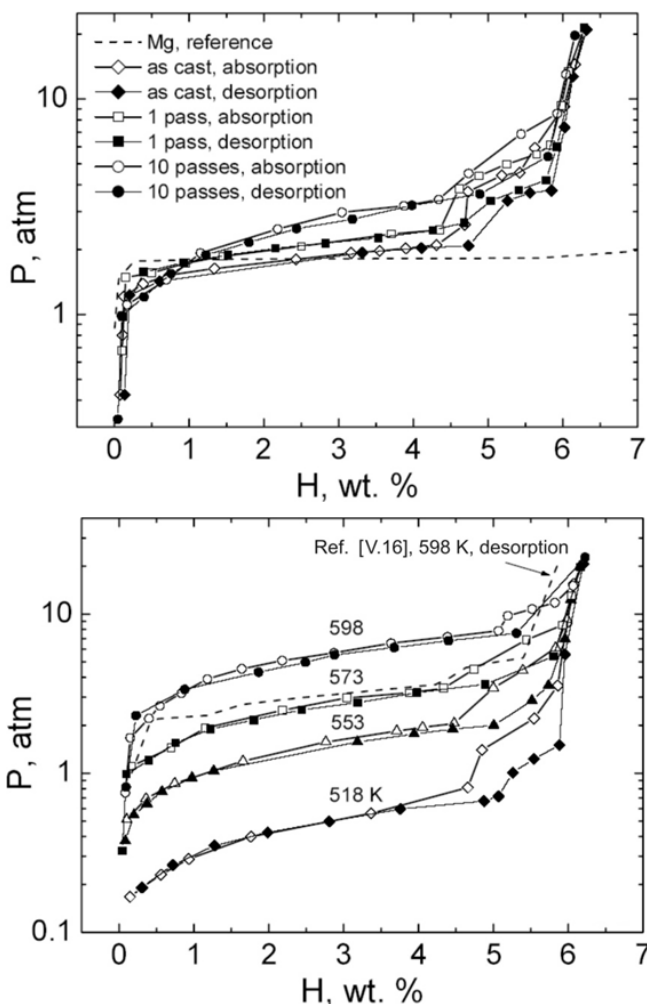
Fig. V.3. PCT diagrams of as cast and ECAP processed samples at 300 °C (top) and PCT diagrams of the sample processed by 10 ECAP passes at different temperatures (bottom)

The reason for such behavior and for the increase of hydrogen absorption/desorption pressure of Mg-related pressure plateau is the chemical inhomogeneity of the supersaturated solid solution of Ni in Mg formed in ECAPed alloys. It is known that Ni, as one of the catalytic elements, weakens the Mg-H bond, which is the reason, why "naturally" created Mg_2Ni phase retains favorable hydrogenation properties. The same function is accomplished by excess

substitutional atoms of Ni in Mg, when hydrogen absorption/desorption pressures of Mg(Ni)H are higher than those for MgH$_2$. For the tilt in pressure plateaus in the low-H part is the initial inhomogeneity in Ni distribution in ECAPed samples responsible as well. Since the rasped particles due to the initial material obtained the same inhomogeneity, the small fragments formed after hydrogenation inherited the differences in the average Ni contents. These differences cannot be leveled of by diffusion at high temperatures during hydrogenation cycling because they are largely physically detached from each other. For a given hydrogenation temperature the grains with lowest Ni content are the first to absorb hydrogen, those with higher Ni concentration doing it slower and after the new hydrogen is added into the system.
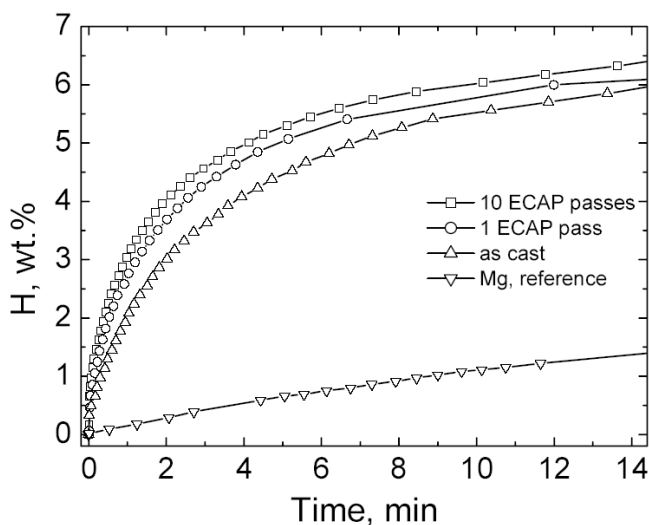

Fig. V.4. Kinetics of hydrogen desorption at 300 °C in as cat and ECAP processed samples. The data for pure coarse grained Mg are shown for comparison.

Fig. V.4 shows the kinetics of hydrogen desorption from ECAPed and as cast alloys at 300 °C. For 10 ECAP passes sample it takes only 5 minutes to desorb 5.5 wt.% of hydrogen, which is almost half so much compared with as cast sample. In Fig. V.5 is shown, that the pressures of hydrogen achieved during desorption are higher for ECAP processed sample than for as cast sample over the whole desorption process.
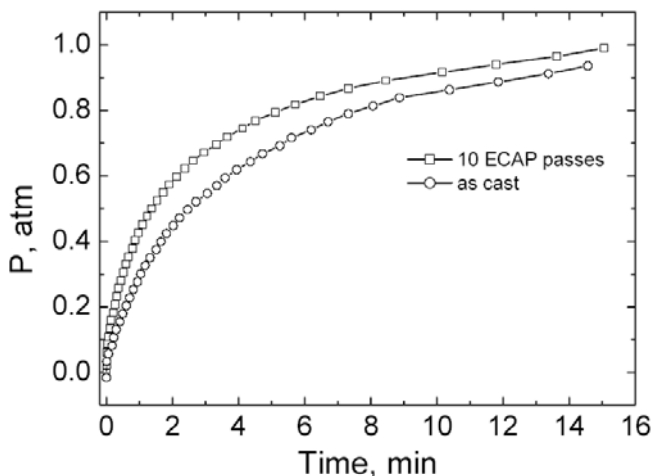
Fig. V.5. Time dependence of hydrogen pressure in desorption volume for the as cast sample and the sample processed by 10 ECAP passes.

The comparison of PCT isotherms at 300 °C for as cast and ECAPed alloys shows that ECAP does modify both the thermodynamics and kinetics of hydrogen-metal interaction. The result of it is that ECAP can outperform such techniques as a more traditional high-energy ball milling (HEBM) for ZK60 [V.15] or melt spinning method used to produce nanocrystalline Mg-Ni alloy of a close chemical composition [V.16] in improving of the hydrogen storage capabilities.

V.5.   Summary

The ECAP was successfully applied to as cast Mg-Ni alloy. 10 ECAP passes resulted in a homogeneous microstructure with sub-micrometer Mg and Mg_2Ni grains. After ECAP processing it was found, that the Mg phase was supersaturated with Ni and some excess of Mg atoms existed in small Mg_2Ni grains.

The hydrogenation properties of the obtained through ECAP ultrafine grain two-phase Mg-Ni alloy were considerably enhanced. A significant acceleration of the kinetics of hydrogen desorption and an increase in equilibrium plateau hydrogen pressure by more than 50% in the PCT diagrams were observed.

Literature:

[V.1]   L. Zaluski, A. Zaluska, J.O. Ström-Olsen, J. Alloys Comp., 253-254 (1997) p. 70

[V.2]   L. Zaluski, A. Zaluska, J.O. Ström-Olsen, J. Alloys Comp., 288 (1999) p. 217

[V.3]   L. Zaluski, A. Zaluska, J.O. Ström-Olsen, J. Alloys Comp., 289 (1999) p. 197

[V.4]   T. Spassov, U. Köster, J. Alloys Comps. 287 (1999) p. 243

[V.5]   W. Oelerich, T. Klassen, R. Bormann, Mat. Trans., 42 (2001) p. 1588

[V.6]   N. Hanada, T. Ichikawa, S. Orimo, H. Fujii, J. Alloys Comp., 366 (2004) p. 269

[V.7]   V. Skripnyuk, E. Buchman, E. Rabkin, Y. Estrin, M. Popov, and S. Jorgensen, J. Alloys Comp. (in press; on-line details: *doi:10.1016/j.jallcom.2006.07.030*)

[V.8]   T.B. Massalski, H. Okamoto, P.R. Subramanian, L. Kacprzak (Eds.), Binary Alloys Phase Diagrams, ASM International, (1990)

[V.9]   A. Yamashita, Z. Horita, T.G. Langdon, Mater. Sci. Eng., A 300 (2001) p. 142

[V.10] M. Mabuchi, K. Ameyama, H. Iwasaki, K. Higashi, Acta mater., 47 (1999) p. 2047

[V.11] L. Jin, D. Lin, D. Mao, X. Zeng, W. Ding, Mater. Lett., 59 (2005) p. 2267

[V.12] Y. Miyahara, K. Matsubara, Z. Horita, T.G. Langdon, Metall. Mater. Trans., A36 (2005) p. 1705

[V.13] Yu. Ivanishenko, W. Lojkowski, R.Z. Valiev, H.-J. Fecht, Acta mater., 51 (2003) p. 5555

[V.14] R.Z. Valiev, R.K. Islamgaliev, I.V. Alexandrov, Progr. Mater. Sci., 45 (2000) p. 203

[V.15] V. Skripnyuk, E. Rabkin, Y. Estrin, R. Lapovok, Acta mater., 52 (2004) p. 405

[V.16] M. Tsukahara, K. Takahashi, A. Isomura, T. Sakai, J. Alloys Comp., 265 (1998) p. 257

VI.   Conclusions

New Mg alloys were effectively undergone to the severe plastic deformation (SPD) due to high pressure torsion (HPT) and equal channel angular pressing (ECAP). ECAP at different temperatures was carried out on the AZ31 and Mg-Ni alloys. After the processing mechanical properties and microstructure were studied, with following results:

HPT was performed on the perspective alloys of Mg-Sm and Mg-Al-Ca systems. The effect of the age-hardening was studied on both alloys. It was shown, that the HPT considerably improves the microhardness of the alloys. The additional aging at 175 °C for Mg-Al-Ca and 200 °C for Mg-Sm alloy provides further microhardness increase with the maximum observed for the samples in quenched condition prior to SPD.

The ECAP at 300 °C of different states of Mg-Al-Ca alloy showed the significant increase of the mechanical properties. The after-deformation aging revealed favorable effect on the strength properties for the material in cast, extruded and ECAPed conditions at room temperature. The yield stress was increased up to 190 MPa in the pre-extruded state followed by ECAP and additional aging. The ductility of the ECAPed samples was superior over the other states and reached 11% and 25% at room and elevated temperatures, respectively.

The ECAP at 220 °C with back pressure showed very high values of microhardness for both alloys, which were much higher than after extrusion or after ECAP at 300 °C.

The microstructure was sufficiently refined, compared to the cast condition. After the ECAP at 300 °C the sub-micron structure was formed, with the grain size of 1-3 µm for Mg-Sm and 2-5 µm for Mg-Al-Ca alloy. Further grain refinement was observed after the ECAP processing at 220 °C with back pressure. The grain size of 200-600 nm was obtained for Mg-Sm, and 300-800 nm for Mg-Al-Ca alloy.

The microhardness measurements of the ECAPed samples at 220 °C revealed the increase of microhardness in 1.8 times for Mg-Sm and in 1.5 times for Mg-Al-Ca alloy in comparison to the values obtained after extrusion or ECAP at 300 °C.

The high values of microhardness after the SPD are stable up to 200-250 °C and they remain still higher than those of the material without SPD.

ECAP at different temperatures was performed on the AZ31 alloy in different states. The sample processed by ECAP at 200 °C attained the maximum elongation to failure of ~560%. The ECAP at 150 °C with back pressure resulted in the record elongation of 1215% for this alloy.

For both states after different ECAP the optimum testing temperature and initial strain rate were found to be 350 °C and $\dot{\varepsilon} = 10^{-4}\,s^{-1}$. The elongation to failure increases with the increase of the testing temperature and decrease of the strain rate.

The grain size was reduced down to ~2 µm after the ECAP processing at 200 °C and down to ~500 nm after ECAP at 150 °C with back pressure. The bi-modal grain structure was obtained after the ECAP at lower temperature. The grain size remained reasonably stable for both states due to the annealing at 350 °C for periods longer than 24 hours.

Up to 10 ECAP passes were carried out on the Mg-Ni alloy. The result was a homogeneous microstructure with sub-micrometer Mg and Mg_2Ni grains. Due to SPD via ECAP the Mg phase was supersaturated with Ni and some excess of Mg atoms was detected in small Mg_2Ni grains.

The hydrogenation properties were significantly enhanced. A considerable acceleration in the kinetics of hydrogen desorption and an increase in equilibrium plateau of hydrogen pressure by more than 50% were observed.

In this work the effect of ECAP processing was shown to provide a significant improvement not only for the mechanical properties, but also for some physical ones. The role of the ECAP temperature on the mechanical properties and superplasticity was studied and the advantage of the ECAP tool equipped with back pressure was presented. The properties of ECAPed materials may differ dramatically depending on the processing parameters, sometimes leading to the erroneous assessment of the poor ECAP potential regarding the enhancement of diverse properties. Though, it is very important to optimize the ECAP tool and choose thoroughly the processing parameters not only for the group of alloys, but for each peace of material considering its initial microstructure and the way it was produced.

VII. Lebenslauf

<u>Persönliches</u>

Mikhail Popov

Staatsangehörigkeit: russisch

Geburtstag: 25.12.1981

Geburtsort: Tynda

<u>Ausbildung</u>

1987 – 1998	Technisches Lyzeum Nr.8, Tynda, Abitur
1998 – 2004	Moskauer Institut für Stahl und Legierungen
	Studium Metallphysik, Abschluss Dipl.-Ing.
2002 – 2004	TU Clausthal
	Studium Werkstoffwissenschaften
	Abschluss Dipl.-Ing.
10/2007	Promotion zum Dr.-Ing. TU Clausthal

<u>Berufliche Tätigkeit</u>

2002 – 2004	Institut für Werkstoffkunde und Werkstofftechnik,
	TU Clausthal, wissenschaftliche Hilfskraft
2004 – 2007	Institut für Werkstoffkunde und Werkstofftechnik,
	TU Clausthal, wissenschaftlicher Mitarbeiter
Ab 2008	Robert Bosch GmbH

Bisher sind erschienen:

Band X / yy

X: 1   Metallurgie und Werkstoffumformung
       2   Polymerwerkstoffe und Werkstofftechnik
       3   Werkstoffkunde und Werkstofftechnik
       4   Nichtmetallisch-anorganische Werkstoffe

yy: fortlaufende Nummer